

1-1-2007

## A study of voltage regulation and islanding associated with distributed generation

Chensong Dai  
*University of Nevada, Las Vegas*

Follow this and additional works at: <https://digitalscholarship.unlv.edu/rtds>

---

### Repository Citation

Dai, Chensong, "A study of voltage regulation and islanding associated with distributed generation" (2007). *UNLV Retrospective Theses & Dissertations*. 2763.  
<http://dx.doi.org/10.25669/o1qk-cj6y>

This Dissertation is protected by copyright and/or related rights. It has been brought to you by Digital Scholarship@UNLV with permission from the rights-holder(s). You are free to use this Dissertation in any way that is permitted by the copyright and related rights legislation that applies to your use. For other uses you need to obtain permission from the rights-holder(s) directly, unless additional rights are indicated by a Creative Commons license in the record and/or on the work itself.

This Dissertation has been accepted for inclusion in UNLV Retrospective Theses & Dissertations by an authorized administrator of Digital Scholarship@UNLV. For more information, please contact [digitalscholarship@unlv.edu](mailto:digitalscholarship@unlv.edu).

A STUDY OF VOLTAGE REGULATION AND ISLANDING  
ASSOCIATED WITH DISTRIBUTED GENERATION

by

Chensong Dai

Bachelor of Electrical Engineering  
Tsinghua University, China  
1997

Master of Electrical Engineering  
Nanjing Automation Research Institute, China  
2000

A dissertation submitted in partial fulfillment  
of the requirements for the

**Doctor of Philosophy Degree in Electrical Engineering**  
**Department of Electrical and Computer Engineering**  
**Howard R. Hughes College of Engineering**

**Graduate College**  
**University of Nevada Las Vegas**  
**December 2007**

UMI Number: 3302350

### INFORMATION TO USERS

The quality of this reproduction is dependent upon the quality of the copy submitted. Broken or indistinct print, colored or poor quality illustrations and photographs, print bleed-through, substandard margins, and improper alignment can adversely affect reproduction.

In the unlikely event that the author did not send a complete manuscript and there are missing pages, these will be noted. Also, if unauthorized copyright material had to be removed, a note will indicate the deletion.

**UMI**<sup>®</sup>

---

UMI Microform 3302350

Copyright 2008 by ProQuest LLC.

All rights reserved. This microform edition is protected against unauthorized copying under Title 17, United States Code.

ProQuest LLC  
789 E. Eisenhower Parkway  
PO Box 1346  
Ann Arbor, MI 48106-1346



**Dissertation Approval**  
The Graduate College  
University of Nevada, Las Vegas

November 16, 20 07

The Dissertation prepared by

Chensong Dai

**Entitled**

"A Study of Voltage Regulation and Islanding Associated  
with Distributed Generation"

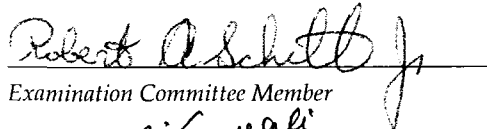
is approved in partial fulfillment of the requirements for the degree of

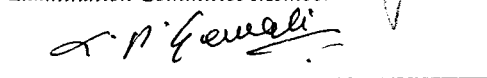
Ph.D. in Electrical Engineering

  
Examination Committee Chair

  
Dean of the Graduate College

  
Examination Committee Member

  
Examination Committee Member

  
Graduate College Faculty Representative

## ABSTRACT

### **A Study of Voltage Regulation and Islanding Associated with Distributed Generation**

by

Chensong Dai

Dr. Yahia Baghzouz, Examination Committee Chair  
Professor of Electrical & Computer Engineering  
University of Nevada, Las Vegas

Distributed generation (DG) is increasingly spreading in the form of solar power, wind power, and fuel cell power. These DGs are connected to the power grid in order to benefit the investors for their economical efficiency and reliability. However, the introduction of DGs, especially at a high level of penetration, brings hidden problems to the conventional power distribution system. The conventional power distribution system has only one direction for the power flow, i.e., from the substation to the end user. This situation may not hold with the introduction of DGs because the power flow may reverse direction in some parts of the feeder. This dissertation will focus on two major problems induced by the introduction of DG: the voltage regulation and the islanding phenomenon.

The study shows the introduction of A DG may cause an over-voltage problem in some segment along the distribution line. The level of over-voltage depends on the size and location of the DGs. Furthermore, DGs are known to impair the operation of

conventional voltage regulation methods, and the study shows that the LTC transformer may be “fooled” by a DG and fails to react to an under-voltage in some cases. The study also shows that switched capacitors can cause an over-voltage if their controls are not modified after introducing DG’s into the feeder. The study reveals the necessity to re-coordinate the control of LTC transformer and the switched capacitors with the introduction of DG units.

The introduction of DG may also cause the islanding phenomenon when the grid power trips off. The DG may continue to supply power to the local load during a utility outage. This situation is of great concern to the utility crew when restoring power. According to a national electrical standard, every DG must shut down in case of grid power loss. The study builds a detailed dynamic model of a grid-connected inverter in a MATLAB/SIMULINK environment. The model simulates the dynamic change in voltage, current, real and reactive power of the DG’s output under various conditions, and simulates the relay action due to over-voltage and under-voltage (OV/UV) and over-frequency and under-frequency (OF/UF). It gives a sound and easy tool to the study of the DG’s dynamics. Based on this model, a novel anti-islanding scheme is present and verified. Also presented are some field tests on the behaviors of two grid-tied PV systems that are equipped with anti-islanding schemes in case of grid outage.

## TABLE OF CONTENTS

ABSTRACT.....	iii
LIST OF FIGURES .....	vii
NOMENCLATURE.....	ix
ACKNOWLEDGEMENT .....	x
<b>CHAPTER 1 INTRODUCTION OF DISTRIBUTED GENERATION .....</b>	<b>1</b>
1.1 A Brief History of DG .....	4
1.2 Potential Benefits of Distributed Generation.....	5
1.3 The Factors Impede Distributed Generation Expansion.....	7
1.4 Undertaking Research on Distributed Generation.....	10
<b>CHAPTER 2 IMPACT OF DG ON VOLTAGE PROFILE ALONG DISTRIBUTION FEEDERS .....</b>	<b>12</b>
2.1 Voltage Profile on Feeders with Uniformly Distributed Loads .....	13
2.2 Voltage Profile on Feeders with Concentrated Loads.....	17
2.3 Summary.....	19
<b>CHAPTER 3 IMPACT OF DG ON VOLTAGE REGULATION IN FEEDERS EQUIPPED WITH LTC TRANSFORMERS.....</b>	<b>21</b>
3.1 Voltage Profile on Feeders Equipped with LTC Transformer .....	22
3.2 Critical DG Size and Location.....	25
3.3 Summary.....	26
<b>CHAPTER 4 IMPACT OF DG ON VOLTAGE REGULATION IN FEEDERS WITH SWITCHED CAPACITORS.....</b>	<b>28</b>
4.1 Assumption of Scenario of Distribution System with DG .....	29
4.2 Capacitor Control and DG Type .....	30
4.3 Approximate Voltage Profile with DG and Capacitor Control.....	32
4.4 Impact of DG and Switched Capacitor on Voltage Regulation .....	36
4.5 Summary.....	37
<b>CHAPTER 5 NUMERICAL EXAMPLE OF THE IMPACT OF DG ON VOLTAGE REGULATION.....</b>	<b>38</b>
5.1 Case I: Impact of DG on Voltage Profile on Feeder with Fixed Substation Voltage .....	40

5.2	Case II - Impact of DG on Voltage Regulation with LTC Transformer Action.....	43
5.3	Case III - Impact of DG on Voltage Regulation with Switched Capacitors .....	46
5.4	Summary.....	49
CHAPTER 6	ISLANDING STUDIES OF INVERTER-BASED DG .....	51
6.1	Review of Anti-islanding Techniques.....	52
6.2	Construction of MATLAB Model for the Inverter-Based DG .....	56
CHAPTER 7	ISLANDING SIMULATION AND FIELD TEST RESULTS.....	67
7.1	Islanding Simulation.....	67
7.2	Islanding Field Tests .....	76
CHAPTER 8	CONCLUSION .....	84
APPENDIX	DEDUCTION OF EQUATION 2-2 .....	86
APPENDIX II	MATLAB SIMULINK MODEL FOR THE GRID-TIED PV SYSTEMS .....	89
APPENDIX III	FIELD TEST PV SYSTEMS AND EQUIPMENTS.....	94
BIBLIOGRAPHY	.....	98
VITA	.....	104

## LIST OF FIGURES

Fig. 1-1	Classic Electricity Paradigm – The Centralized Power Model.....	3
Fig. 1-2	Distributed Generation (DG) Electricity Paradigm – Distributed/Onsite Generation .....	3
Fig. 2-1	Real Power Flow along a Uniformly Loaded Feeder .....	14
Fig. 2-2	(a) Real Power Flow & (b) Reactive Power Flow along a Uniformly Loaded Feeder with Two DG Units .....	17
Fig. 2-3	(a) Feeder with Concentrated loads, (b) Real Power Flow without DG, (c) Power Profile with DG at Node $k$ .....	18
Fig. 3-1	Voltage Regulation by LTC Transformer with LDC .....	22
Fig. 3-2	Active and Reactive Power Profile along Feeder without and with DG at Distance $d$ from Substation .....	23
Fig. 4-1	(a) Feeder with DG and Switched Capacitors; (b) Daily Power Curves with Switched Capacitors and DG .....	33
Fig. 5-1	Radial Distribution Circuit .....	39
Fig. 5-2	Voltage Profile without & with DG Supplying 8MW at Different PF (with Uniform Loads).....	40
Fig. 5-3	Maximum DG Real Power Output as Function of Distance from Substation .....	41
Fig. 5-4	Voltage Profile without & with DG Supplying 8MW at Different PF (with Concentrated Loads) .....	42
Fig. 5-5	Percent Errors of Node Voltages Obtained Uniform Loads and Concentrated Loads Methods w/o and with DG at Node 5.....	42
Fig. 5-6	Feeder Voltage Profile at Different Load Levels Prior to DG Installation .....	43
Fig. 5-7	Voltage Profile with 5 MW DG Installed at Different Locations during Peak Load.....	45
Fig. 5-8	Voltage Profile for Different DG Sizes Installed at 1 mi from Substation during Peak Load.....	45
Fig. 5-9	(a) Feeder Real Power; (b) Feeder Reactive Power; (c) Ambient Temperature during Peak Demand.....	47
Fig. 5-10	Voltage Profile before and after Capacitor Switching (w/o DG) .....	48
Fig. 5-11	Time Variation of Some Feeder Node Voltages (w/o DG) .....	48
Fig. 5-12	Voltage Profile before and after Capacitor Switching (with 2 MW DG at Node 7) .....	49
Fig. 6-1	Grid-connected PV System with Local Load .....	55
Fig. 6-2	Block Diagram of the Grid-tied PV System .....	57
Fig. 6-3	(a) Relay Control Scheme and (b) Relay Control Signal Generator .....	59
Fig. 6-4	Breaker Control Scheme.....	60
Fig. 6-5	Circuit to Determine the Control Equations for Voltage Mode PWM.....	61

Fig. 6-6	Circuit to Determine the Control Equations for Current-Mode PWM.....	63
Fig. 6-7	PWM Control Waveform Generator .....	65
Fig. 7-1	Inverter Terminal Voltage, Frequency & Output Real and Reactive Power (with Relay Set to Non-function).....	68
Fig. 7-2	Inverter Terminal Voltage, Frequency & Output Real and Reactive Power and Relay Control Signal (with Relay Set to Function).....	69
Fig. 7-3	Inverter Terminal Voltage, Frequency & Output Real and Reactive Power and Relay Control Signal (with Relay Set to Function).....	70
Fig. 7-4	Inverter Terminal Voltage, Frequency & Output Real and Reactive Power and Relay Control Signal (with Relay Set to Function).....	71
Fig. 7-5	Inverter Terminal Voltage, Frequency & Output Real and Reactive Power and Relay Control Signal (with Relay Set to Function).....	72
Fig. 7-6	Inverter Terminal Voltage, Frequency & Output Real and Reactive Power and Relay Control Signal (with Relay Set to Function).....	73
Fig. 7-7	Inverter Terminal Voltage, Frequency & Output Real and Reactive Power and Relay Control Signal (Capacitor Switching in 0.167s Period).....	75
Fig. 7-8	Schematic Diagram of Test Circuit .....	77
Fig. 7-9	Phase Voltage Waveforms during Event A.1 .....	79
Fig. 7-10	Phase Voltage Waveforms during Event A.2.....	80
Fig. 7-11	Phase Voltage Waveforms during Event A.3.....	80
Fig. 7-12	Phase Voltage Waveforms during Event B.1 .....	82
Fig. 7-13	Phase Voltage Waveforms during Event B.2.....	82
Fig. 7-14	Phase Voltage Waveforms during Event B.3.....	83
Fig. I-1	Circuit with One Lumped Load.....	86
Fig. I-2	Phasor Diagram of Voltage Drop.....	86
Fig. I-3	Real Power Flow Profile along the Distribution Line with Uniform Loads .....	87
Fig. I-4	Equivalent Circuit with Two Lumped Loads .....	87
Fig. II-1	Grid-Tied PV System .....	90
Fig. II-2	Relay Control Signal Generator .....	91
Fig. II-3	PWM Control Signal Generator .....	92
Fig. II-4	Simulation Monitor .....	93
Fig. III-1	PV System A: Daystar 1 Solar Facility .....	94
Fig. III-2	PV System B: Amonix Concentrating PV System .....	95
Fig. III-3	Load Bank .....	95
Fig. III-4	Measuring Point and Utility Disconnect Switch .....	96
Fig. III-5	Current Probes.....	96
Fig. III-6	Transient Recorder .....	97

## NOMENCLATURE

CHP	Combined Heat and Power
CCHP	Combine Cooling, Heat and Power
DG	Distributed Generation
DOE	Department of Energy
GMD	Geometrical Mean Distance
LTC	Load Tap Changer
LDC	Line Drop Compensator
PF	Power Factor
PI	Proportional-Integral
PWM	Pulse Width Modulation
PV	Photovoltaic
pu	per unit
SCADA	Supervisory Control and Data Acquisition
THD	Total Harmonic Distortion

### From Chapter 2 to Chapter 5:

$d$	distance from substation (mi)
$l$	length of distribution line (mi)
$R, X$	resistance and inductance of distribution line per mile. ( $\Omega$ /mi)
$R_{a,b}, X_{a,b}$	total resistance and inductance of segment node a to node b of the distribution line. ( $\Omega$ )
$P_0, P_d$	real power flow at substation / distance $d$ from substation (MW)
$Q_0, Q_d$	reactive power flow at substation / distance $d$ from substation (MVAR)
$V_0, V_d$	voltage magnitude at substation / distance $d$ from substation (pu)
$V_b$	nominal voltage magnitude of distribution system (kV)
$VD_d$	voltage drop from substation to point distance $d$ (pu)
$VD_{a-b}$	voltage drop from node a to node b (pu)

### From Chapter 6 to Chapter 7

$R, X$	resistance and inductance ( $\Omega$ )
$P_S, P_D, P_L$	real power of the grid, DG, load (kW)
$Q_S, Q_D, Q_L$	reactive power of the grid, DG, load (VAR)
$V_{PV}$	voltage magnitude at PV system output terminal (V)
$\omega$	radial frequency (radian/s)
$\delta$	angle between two node (radian)

## ACKNOWLEDGEMENTS

I would like to thank my advisor Dr. Yahia Baghzouz for his help and support to complete this project and throughout the Ph.D. program.

I feel grateful to committee members who agreed to take the time to evaluate my dissertation.

And I would also like to give special thanks to Dr. Yingtao Jiang and my parents, who helped me to get over my difficult time. Only with their support all the time comes this dissertation to the final.

## CHAPTER 1

### INTRODUCTION OF DISTRIBUTED GENERATION

Electric power is essential to modern society. Today 40% of the energy consumption in US is used to produce electricity [1]. After more than 100 years of development, the America's electric system has grown up to a very large sophisticated system. This bulk system includes about 10,000 power plants, about 157,000 miles of high voltage (>230kV) electric transmission lines, and enormous distribution networks spreading almost all over the continent providing electric power to 131 million America's electricity consumers. However, the electrical U.S. system is aging and becoming more congested. Soon it will be incapable of meeting the future energy needs without operational changes and substantial capital investment.

In order to meet the increasing and changing requirements from electrical consumers, the Department of Energy (DOE) recently proposed a vision of the future electric system, i.e., "Grid 2030" [1]. The future system builds on the existing electric infrastructure and applies new technologies, tools and techniques to develop a new architecture for the electric grid, which will be a high-efficient network of both power delivery and market operations, and a high-quality network that provides secure source of electricity to America.

The current model for electricity generation and distribution is dominated by the central power station model, the classic power paradigm as illustrated in Fig. 1-1 [3]-[4].

These centralized power plants are typically based on the combustion of fossil fuels (coal, oil and natural gas) or nuclear reaction. The centralized power models require that customers acquire electricity through distribution networks and transmission networks, which are becoming congested at multiple locations. In addition to transmission problems, centralized power plants have many other disadvantages, such as greenhouse gas emission, nuclear waste, power loss over lengthy transmission lines, and security related issues [2]-[5].

In the future electric system, distribution networks will evolve from current passive networks to active networks which will include a number of different types of distributed generation resources, such as fuel cells, reciprocating engines, distributed gas turbines and micro-turbines. Fig. 1-2 shows an example of future DG model, where the customers are provided by distributed or onsite generation with fully integrated network management. However, more and more problems are emerging as more and more DG units are tied to the grid. There is often a lack of familiarity with DG technology, which has contributed to the perception of added risks and uncertainties, also to a lack of standard data, models, and analysis tools for evaluating DG, or standard practices for incorporating DG into electric system planning and operations [2]. Nevertheless, DG offers potential benefits to electric system planning and operations. Using DG to meet local system needs can greatly reduce the congestion in the transmission networks and add up to improvements in overall electric system reliability. Also DG can be used to decrease the vulnerability of the electric system to threats from terrorist attacks, and other forms of potentially catastrophic disruptions.

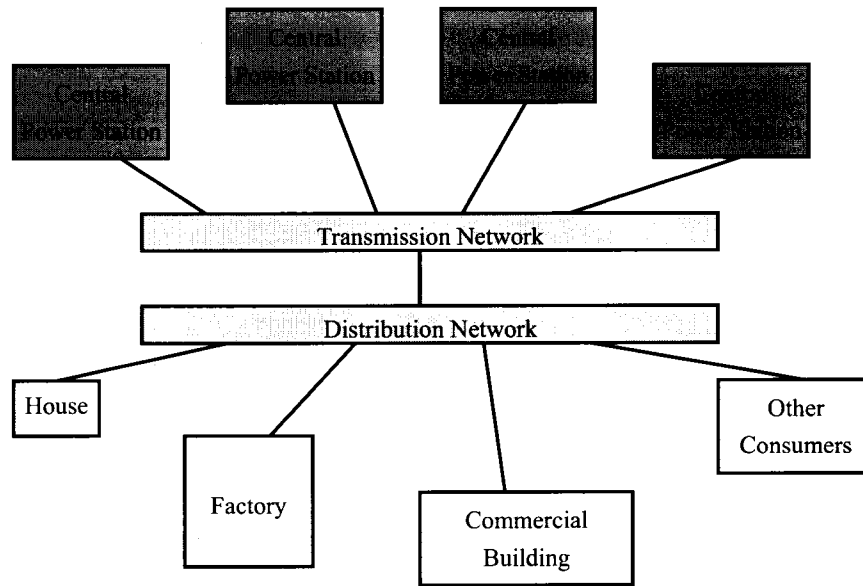


Fig. 1-1: Classic Electricity Paradigm – The Centralized Power Model.

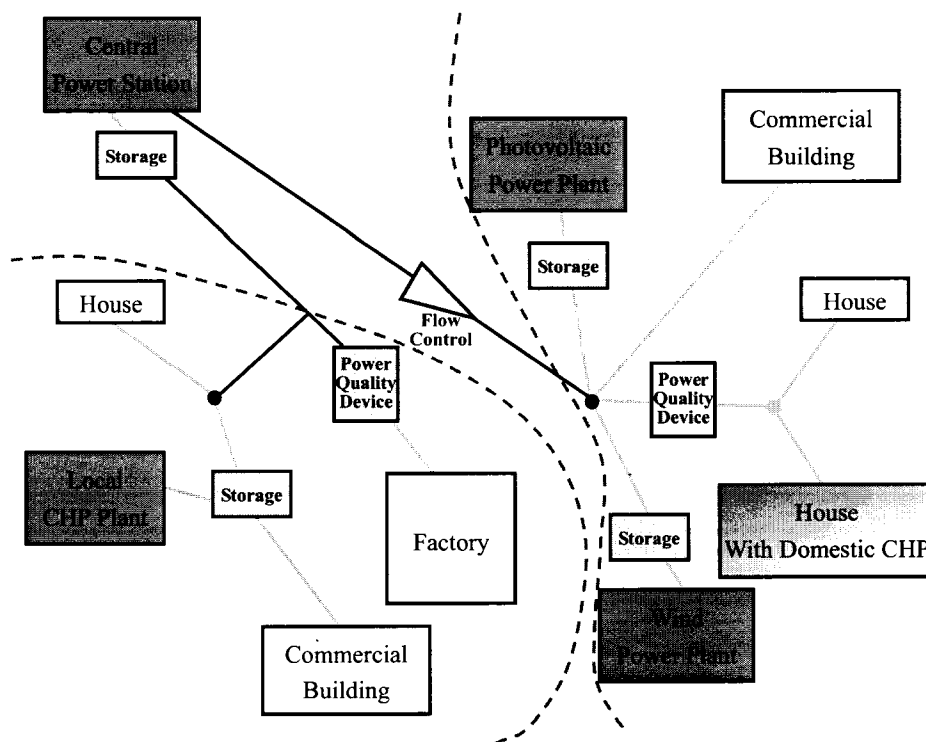


Fig. 1-2: Distributed Generation (DG) Electricity Paradigm – Distributed/Onsite Generation

## 1.1 A Brief History of DG

Distributed Generation is a new concept to traditional electricity generation and electricity market. DG is commonly referred to as on-site generation, dispersed generation, embedded generation, decentralized generation, decentralized energy or distributed energy generation. The IEEE defines distributed generation as the generation of electricity by facilities that are sufficiently smaller than central generating plants so as to allow interconnection at nearly any point in a power system [9]. This definition includes such technologies as photovoltaic; small wind; small biomass; small combined heat and power (CHP) or small cogeneration; small combined cooling, heat and power (CCHP); and small non-CHP systems [8].

The idea of DG is not new at all. In the very initial stages of the electric power industry in the early 20<sup>th</sup> century, all energy requirements were supplied near or at their point of use [2]. Technology advances and other power industry economy progresses lead the power industry converging to the network of gigawatt-scale thermal power plants located far from the urban centers that we know today. At the same time, this centralized generation system was evolving, some customers found it technically and economically necessary to install and operate their own electric power units. These “traditional” forms of DG work mainly as backup power or emergency power during outages.

The new era of energy efficient and renewable DG came to the electric power system application since when the US Congress enacted the Public Utility Regulatory Policies Act of 1978 (PURPA) [2][4]. PURPA and a series of laws after this gradually removed the impediments to the development of DG. In the past few decades, distributed generation greatly extends its application area. Now it works not only as backup power

but mainly as grid-connected power. The recent advances in material technology greatly expanded the application of distributed generation. Now the major members in DG applications are those new forms of DG, or “modern” DG, that use renewable resources like photovoltaics, wind, and fuel cells. Currently, there are about 12 million DG units installed across America, with a capacity of about 200 GW [2], and this number is expected to grow rapidly in the future.

## 1.2 Potential Benefits of Distributed Generation

The interest in distributed generation in the past decades is induced by the potential benefits of distributed generation to the electricity system in technical and economic ways, at both the utility and customer sides. Research studies concluded that distributed generation technology can bring benefits far beyond the electricity network. It can also bring benefits to the whole society in terms of environmental impact and security insurance [2][4][5]. DOE published a report in 2007 [2] summarizing the potential benefits of distributed generation in 8 major points.

- ◆ *DG can increase the electric system reliability.* DG can improve the electric system reliability by both direct and indirect ways. In a direct way, DG can add to supply diversity and thus lead to the improvements in overall system adequacy. In an indirect way, DG has the potential to reduce outages caused by overloaded utility equipments.
- ◆ *DG can reduce peak power requirements (peak shaving).* The national average load factor is about 55%. This means that electric system assets, on average, are used about half the time [1]. The installation and use of DG systems by customers and/or by utilities can produce reductions in peak load requirements, and thus

increase the load factor. This means DG can increase the average using efficiency of overall electric system assets. Since most investment decisions on new plants or equipments are based on the peak load requirements, reductions in peak load can displace or defer capital investments.

- ◆ *DG can provide ancillary services like reactive provider, supplement reserve, etc.* DG can be used to provide ancillary services, particularly those that are needed locally, such as reactive power, voltage support, but also those that contribute to the reliable operation of the entire system, such as back-up supplies and supplement reserves.
- ◆ *DG can improve power quality.* “Modern” DG systems are usually integrated with energy storage equipments, power electronics components, and power conditioning equipments. These devices are very useful in addressing power quality problems. For example, they can protect sensitive equipments from voltage spikes or sags. They can also reduce the total harmonics distortion (THD) in electric system.
- ◆ *DG can reduce the land use effects and rights-of-way.* Energy generation, transmission, and distribution have an obvious impact on land use. Under certain circumstances, DG can have positive land use benefits, including smaller land mass requirements, saving on acquisition costs, right-of-way, and land retention, and so on. A lot of DG systems are incorporated into buildings, in an engine room, on a rooftop, or immediately adjacent.
- ◆ *DG can reduce the CO<sub>2</sub> emissions and the pollutant emissions.* Power generation accounted in 2004 for 41% of total man-made CO<sub>2</sub> emissions and large proportion

of heavy metals, NO<sub>x</sub>, SO<sub>x</sub> and dust [5]. “Modern” DG systems are using renewable resources or applying recycled energy technology. They can have significant impact on reducing the gas and pollutant emissions, and thus benefit the society on environmental protect and human health improvement.

- ◆ *DG can provide the feasible solution to electrify the remote areas.* DG technology can provide a feasible solution to electrify the remote areas by utilizing the local resources without great impact on the community. Those areas usually have too low population density to justify grid access or connection. DG technology is a far cheaper solution to supply power to those areas than grid extension. A number of micro-grids demonstration projects have been undertaken in the Greek islands [3].
- ◆ *DG can reduce the vulnerability of the electric system to terrorism and provide infrastructure resilience.* DG can improve electric system resilience through its reliance on large numbers of smaller and more geographically disperse power plants, rather than large central station power plants and bulk-power transmission facilities. During times of large-scale power disruptions and outages, DG can continue to provide power to critical facilities.

The above potential benefits are mostly proven by concrete examples [2]. They are the driving forces to distributed generation research and application. DG will continue to be an attractive energy solution to certain customers. And DG will draw more interest of electric system planners and operators, and will be applied more by electric utilities.

### 1.3 Factors That Impede Distributed Generation Expansion

Despite the above potential benefits, there are a number of problems that may impede DG expansion. Currently, rules, regulations, rate-making practices discourage DG

because they impose costs or burdens that reduce financial attractiveness. Also, the benefits of DG often favor the customer side, and the burdens of solving the impacts of DG are mainly carried by the electric utilities. This unbalance also causes the electric system planners and operators to be reluctant to allow more DG integration into their system.

Technically, to achieve the positive benefits of DG, it must be suitably coordinated with the system operating philosophy and feeder design [12]. Otherwise, the introduction of DG will induce a lot of problems to the traditional distribution system, including its regulation mechanism, protective coordination, and unintentional islanding problems. The larger the aggregate DG capacity on a circuit relative to the feeder capacity and demand, the more critical is the coordination with the factors of DG units. Much research work has been done to this subject in the past decade, and many cases have been studied to address the problems introduced by mis-coordinated DG. Meanwhile, a number of solutions and suggestions have been presented to solve or mediate these problems [12]-[21]. The impact of distributed generation to the traditional radial distribution system can be summarized as those points below.

- ◆ *Voltage Regulation and Losses.* Radial distribution systems are normally regulated using load-tap-changing transformers at substations, supplementary line regulators on feeders, and switched capacitors on feeders. The introduction of DG alters the uni-direction of power flow through the radial distribution system. The introduction of DG will deceive the regulator devices and equipments causing them set to a wrong statue in some cases, and sometimes will be unable to coordinate with the equipments under any cases [13]-[21]. The type and severity

of these problems depends on the size and location of the DG units.

- ◆ *Voltage Flicker.* DG may cause noticeable voltage flickers. From a simple perspective, flicker can be the result of starting a machine or a step change in DG output which result in a noticeable voltage change on the feeder. In the case of inverter-based DG, the output voltage may fluctuate significantly as the resource energy intensity changes.
- ◆ *Harmonics.* Distribution generation units may introduce harmonics. The type and severity depends on the power converter technology and interconnection configuration. Fortunately, this problem becomes mediated with the development on the power electronics technology, control technology and material technology. IEEE 519-1992 [31] limits the harmonic current injection of the DG unit interconnected into the grid. And IEEE also made the standard IEEE std. 1547 [32] to set the interconnection between DG units and the grid to desired requirements.
- ◆ *Impact on Short Circuit Levels.* The fault contribution from a single DG unit is normally not large. However, the penetration of DG can be large enough to interfere with the relay devices on the feeder when many small DG units are installed or a few large DG units are installed. In such cases, the fuse-breaker coordination may lose its function. Many papers [51]-[53] have pointed out the impact of DG on relay coordination. It is already known that the re-closer may be not able to coordinate with DG unit(s) with large penetration.
- ◆ *Grounding and Transformer Interface.* Distributed generation must be applied with a transformer configuration and grounding arrangement compatible with the utility system to which it is to be connected. Otherwise, voltage swells and

over-voltages may be imposed on the utility system that damage utility or customer equipment. To avoid these problems, all DG sources on multi-grounded neutral systems that are large enough to sustain an island should present themselves to the utility system as an effectively grounded source.

- ◆ *Islanding*. Islanding occurs when the distributed generation unit(s) continues to energize a portion of the utility system that has been separated from the main utility system. This separation could be due to operation of an upstream breaker, fuse, or automatic sectionalizing switch, or manual switch. Islanding can occur only if the DG unit can sustain the load in the islanded area [22]-[24]. In response to this concern. Much research work has been done to explore the islanding phenomenon induced by DG, and many ideas, designs, and patents are presented as “anti-islanding” techniques. More details on this subject will be discussed on Chapter 6.

#### 1.4 Undertaking Research on Distributed Generation

As mentioned above, significant research work is already reported on DG technology, its benefits and on its negative impacts. The work is still ongoing because of the unsolved emerging related problems. In this dissertation, the study is focused on two major problems induced by DG: the voltage regulation problem and the islanding problem. In the first problem, the impact of a DG unit(s) on the voltage profile in a distribution feeder is analyzed in detail. The presence of an active LTC (Load Tap Changer) transformer with LDC (Line Drop Compensator), and switched capacitor banks is undertaken for the first time. In the second problem, the inverter-based DG is studied in great detail by analyzing the issue of occurrence of islanding under numerous scenarios. A MATLAB-Simulink

model is built to predict the behavior of the inverter-based DG both under balanced and unbalanced power production. Field tests are also conducted on two local inverter-based DGs to verify their behavior during a utility outage.

## CHAPTER 2

### IMPACT OF DG ON VOLTAGE PROFILE

#### ALONG DISTRIBUTION FEEDERS

It is known that DG reduces power loss and releases system capacity, but complicates power distribution system protection coordination. However DG impact on voltage regulation can be positive or negative depending on distribution system and distributed generator characteristics as well as DG location. Since voltage regulation is an important criterion from the electrical service quality point of view, such impact studies attracted quite a bit of attention in recent years [13]-[15]. In particular, when a DG is applied downstream of a voltage regulator or a LTC (Load Tap Changer) transformer equipped with LDC (Line Drop Compensator), it will confuse the regulator into setting a voltage lower than is required for adequate service [12]. This either limits the DG operating range or requires complicated DG-LTC coordination schemes [16]-[19]. While the use of LDC minimizes voltage swings along the feeder, it is not used by a number of utilities due to numerous drawbacks, including difficulty in determining the control point of multiple feeders, changing conditions on the feeder, and potential serious consequences of switched capacitors beyond the regulating point [26].

This chapter analyzes the impact of DG on the voltage profile of distributions circuits where the LTC transformer is not equipped with without LDC, i.e., the voltage is held constant at the substation bus. First, an analytical expression for the voltage profile

along a feeder with uniformly distributed load is derived in terms of the DG power and distance from the substation. The critical DG size that results in maximum permissible voltage at DG location is also derived. The procedure is extended for feeders with multiple DG units and feeders with concentrated loads using simple sequential calculations. The analysis will be illustrated by a numerical example in Chapter 5.

### 2.1 Voltage Profile on Feeders with Uniformly Distributed Loads

In a distribution feeder of length  $l$  with uniformly distributed load, the active and reactive power flow drop linearly with distance  $d$  from the substation as shown in Fig. 2-1 (a), i.e.,

$$U_d = U_0 \left(1 - \frac{d}{l}\right), \dots \dots \dots (U = P, Q) \quad (2-1)$$

The voltage drop in per unit value at point  $d$  can be decomposed into two components: one due to the load downstream, i.e.,  $(P_d, Q_d)$  is lumped at point  $d$ , and one due to the lumped-sum load upstream located at half the distance. These components can be approximated by [26], [27], and the details of the deduction are shown in Appendix I:

$$VD_d = d \frac{RP_d + XQ_d}{V_b^2 V_d} + \frac{d}{2} \frac{R(P_0 - P_d) + X(Q_0 - Q_d)}{V_b^2 V_d} \quad (2-2)$$

where  $R$  and  $X$  represent the feeder resistance and inductive reactance per mile,  $V_b$  and  $V_d$  are the base voltage and the voltage in pu at point  $d$ , respectively. Substituting (2-1) in (2-2) above yields

$$VD_d = V_0 - V_d = \frac{VD_d^a}{V_d} \quad (2-3)$$

where

$$VD_d^a = \frac{1}{V_b^2} (RP_0 + XQ_0) \left( d - \frac{d^2}{2l} \right) \quad (2-4)$$

and  $V_0$  denotes the substation voltage. Solving for  $V_d$  from Eqn. (2-3) results in the following expression:

$$V_d = \frac{1}{2} \left\{ V_0 + \left( V_0^2 - 4VD_d^a \right)^{1/2} \right\} \quad (2-5)$$

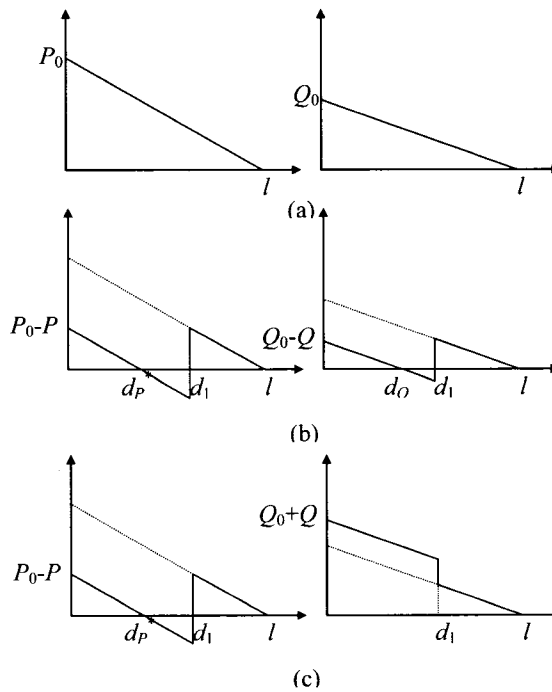


Fig. 2-1: Real Power Flow along a Uniformly Loaded Feeder (a) without DG, (b) with DG with PF Lag, (c) with DG with PF Lead.

Unlike the application of shunt capacitors that affect only the reactive component, installing a DG will affect both components since many types of distributed generators are able to generate both real and reactive powers. The power ( $P_G$ ,  $Q_G$ ) injection at  $d_1$  will counteract both components of the voltage drop in Eqn. (2-2) by producing a “voltage

rise” upstream as shown in Fig. 2-1(b) above. However, if the installed DG operates at a leading power factor, its active and reactive components will have opposite effects as shown in Fig. 2-1(c). The voltage along the feeder is the computed as follows:

For  $d \leq d_l$ ,

$$V_d = \frac{1}{2} \left\{ V_0 + \left( V_0^2 - 4VD_d^b \right)^{1/2} \right\} \quad (2-6)$$

where

$$VD_d^b = VD_d^a - \frac{d(RP_G + XQ_G)}{V_b^2} \quad (2-7)$$

For  $d > d_l$ ,

$$V_d = \frac{1}{2} \left\{ V_{d_l} + \left( V_{d_l}^2 - 4VD_d^c \right)^{1/2} \right\} \quad (2-8)$$

where  $V_{d_l}$  corresponds to the evaluation of Eqn. (2-6) at  $d = d_l$ , and

$$VD_d^c = \frac{(d - d_l)(RP_{d_l} + XQ_{d_l})}{V_b^2} \left\{ 1 - \frac{(d - d_l)}{2(l - d_l)} \right\} \quad (2-9)$$

Note that in Fig. 2-1(b), the injected powers are assumed to be larger than the load downstream of its location. This causes the so-called “zero point” [20] where active (reactive) power flow changes direction, i.e., flows “up-hill” towards the substation to the left of the zero point, and “down-hill” in a conventional way to the right of the zero point. No impact on feeder loading takes place past the DG location. If the injected power is less than the load downstream, there will be no zero point and power simply flows “down-hill” at reduced level up to DG location.

#### 2.1.A. DG Operating Range

The injected powers ( $P_G$ ,  $Q_G$ ) by the placement of a DG at  $d_l$  improves voltage regulation by reducing voltage drop as indicted by Eqn. (2-6). The largest amount of

power generation that will not result in an over-voltage at the DG location can be obtained by setting the voltage at  $d_l$  to the upper permissible limit. This is equivalent to setting the voltage drop in Eqn. (2-7) to zero. The resulting DG powers must satisfy the following equation:

$$RP_G + XQ_G = (RP_0 + XQ_0) \left(1 - \frac{d_l}{2l}\right) \quad (2-10)$$

The maximum real power generated by the DG can be written in terms of the DG operating power factor,

$$P_G = \frac{(RP_0 + XQ_0)(1 - d_l/2l)}{R + X \tan\{\cos^{-1}(PF)\}} \quad (2-11)$$

Note that the maximum generated power is proportional to the total feeder load. This indicates that the DG power generation limit is reduced proportionally with the feeder load unless the LTC transformer is adjusted to a lower voltage at lighter loads.

#### 2.1.B. Multiple DG installations

The above analysis can easily be extended to the case of multiple DG sites along the feeder. To illustrate, Fig. 2-2 shows feeder power flow with two distributed generators (the one at  $d_1$  is shown to be operating at lagging power factor, and one at  $d_2$  is operating at leading power factor). The voltage profile along this line can be computed by previous equations with simple substitutions:

- ◆ For  $d \leq d_1$ , replace  $(P_G, Q_G)$  by  $(P_{G1}+P_{G2}, Q_{G1}+Q_{G2})$  in Eqns. (2-6) and (2-7).
- ◆ For  $d_1 < d \leq d_2$ , replace  $(P_G, Q_G)$  by  $(P_{G2}, Q_{G2})$  and  $V_0$  by  $V_{d1}$  in Eqns. (2-6) and (2-7).

- ◆ For  $d > d_1$ , replace  $V_{d1}$  by  $V_{d2}$ ,  $d_1$  by  $d_2$ , and  $(P_{d1}, Q_{d1})$  by  $(P_{d2}, Q_{d2})$  in Eqns. (2-8) and (2-9).

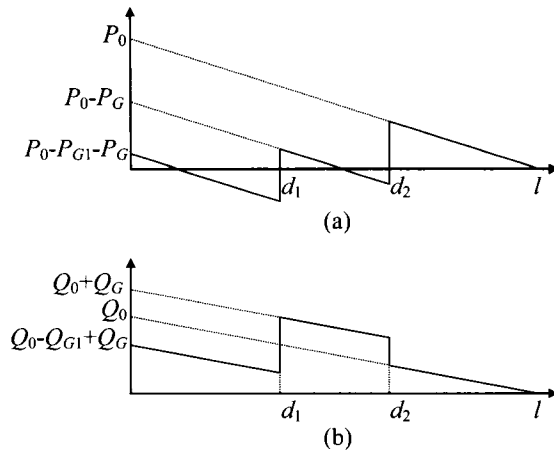


Fig. 2-2: (a) Real Power Flow & (b) Reactive Power Flow along a Uniformly Loaded Feeder with Two DG Units

## 2.2 Voltage Profile on Feeders with Concentrated Loads

The above analysis is limited to situations where the load is uniformly distributed throughout the feeder length, and the feeder size and GMD is constant. Many feeders, however, have uneven concentrated loads at specific locations and the cables may consist of smaller sizes at nodes farther from the substation. These feeders are best represented by the concentrated load model shown in Fig. 2-3(a) where  $(P_i, Q_i)$  represent the load active and reactive power consumption at node  $k$ ,  $k=1, \dots, n$ .

The real and reactive power flow in line segment  $(k-1, k)$  can be approximated by the sum of the sum of the loads connected at nodes  $k$  through  $n$ ,

$$U_{k-1,k} = \sum_{i=k}^n U_i, \dots \dots (U = P, Q) \quad (2-12)$$

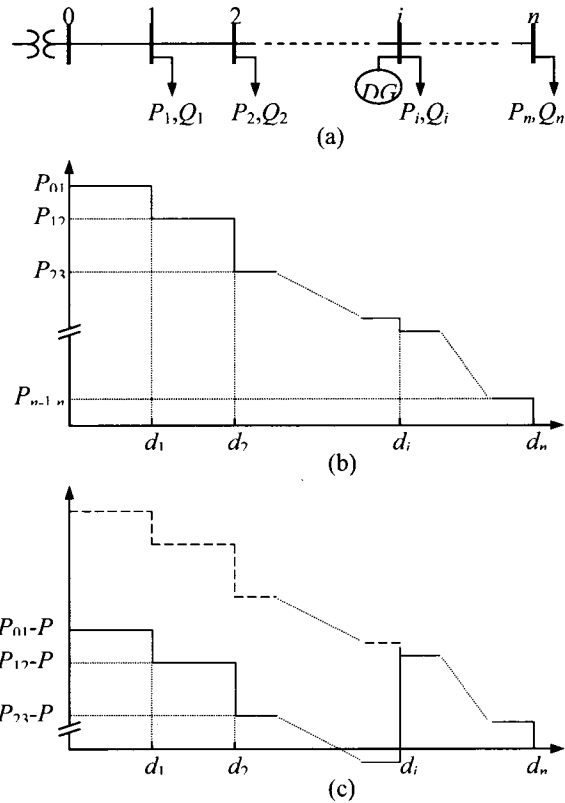


Fig. 2-3: (a) Feeder with Concentrated loads, (b) Real Power Flow without DG, (c) Power Profile with DG at Node  $k$

The resulting power profile is represented by a staircase curve as illustrated in Fig. 2-3(b) which

$$V_k = \frac{1}{2} \left\{ V_{k-1} + \left( V_{k-1}^2 - 4VD_k^d \right)^{1/2} \right\} \quad (2-13)$$

shows only the real power flow curve. Given the fixed voltage  $V_o$  at the substation, the approximate voltage at any node  $k$  can be computed sequentially by

$$VD_k^d = \frac{R_{k-1,k}P_{k-1,k} + X_{k-1,k}Q_{k-1,k}}{V_b^2} \quad (2-14)$$

Herein,  $(R_{k-1,k}, X_{k-1,k})$  represent the resistance and inductive reactance of line segment  $(k-1,k)$ .

Similar to the previous section, power injection by a DG unit at node  $k$  will reduce real power flow in the line segments upstream by  $P_G$  as illustrated in Fig. 2-3(c), and reactive power flow by  $\pm Q_G$  (depending on whether the DG is supplying or absorbing reactive power), while the power flow downstream from the DG remains nearly the same.

$$U_{k-1,k} = -U_G + \sum_{i=k}^n U_i, \dots \dots \dots (U = P, Q) \quad (2-15)$$

Following the same procedure above, the new voltage profile upstream is computed by Eqn. (2-13) after substituting the new power flows of Eqn. (2-15) in Eqn. (2-14). The analysis can also be extended to multiple DG units without much difficulty.

### 2.3 Summary

Installing Distributed Generation units along power distribution feeders may lead to over-voltages due to excessive active and reactive power injection. This chapter proposed a simple analytical method to estimate the voltage profile when placing DG units with specific active and reactive power generation. Assuming that the load is uniformly distributed (in order to lend quick hand calculations) is expected to be sufficiently accurate many feeders. Coordination between DG outputs and LTC tap controls is a necessity in order to allow higher levels of distributed resources. Otherwise, power

injection levels can be severely limited if substation voltage is kept constant by the LTC transformer.

## CHAPTER 3

### THE IMPACT OF DG ON VOLTAGE REGULATION IN FEEDERS EQUIPPED WITH LTC TRANSFORMERS

The previous chapter analyzed the impact of DG on the voltage profile along distribution feeders. It was determined that a DG can cause the voltage to deviate above or below the permissible range in some parts of the feeder, thus resulting in the opposite effect of voltage support, unless careful coordination between the DG and voltage regulation controller is carefully engineered [18]-[19].

This chapter analyzes the possibility of an under-voltage caused by installing a DG unit on a feeder where voltage regulation is controlled by the substation LTC (Load Tap Changing) transformer that is equipped with LDC (Line Drop Compensator) controls. In this a case, the introduction of the DG may confuse the regulator in setting a lower substation transformer secondary voltage than necessary, thus causing excessively low voltages towards the feeder end. The section that follows derives approximate voltage drops along uniformly distributed feeders under the presence of a single DG unit. Simple expressions of maximum DG size at a given location, and minimum distance from the substation a given DG size can be installed, that result in acceptable voltage are derived. The analysis will be illustrated by a numerical example in Chap. 5.

To simplify the analysis, the impact of switched capacitor banks is not considered, and this subject is studied in the next chapter. In addition, DG is considered to operate at

unity power factor, a common practice for inverter-based DG systems, but the analysis can be expanded to include distributed generators that either generate or absorb reactive power without much difficulty.

### 3.1 Voltage Profile on Feeders Equipped with LTC Transformer

Fig. 3-1 shows a distribution feeder of length  $l$  with a uniformly distributed load, where voltage regulation is controlled with the substation LTC transformer with LDC. The resulting voltage profiles along the feeder at full load and half load are also shown in the Fig. 3-1. As the load varies, the regulator adjusts the transformer tap position such that the voltage at the “regulating point” along the feeder is kept constant.

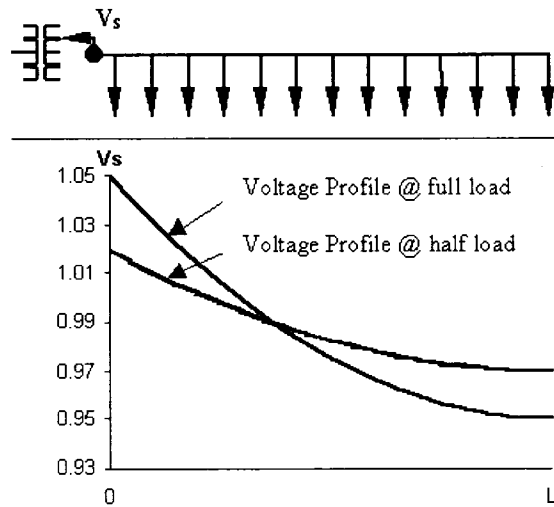


Fig. 3-1: Voltage Regulation by LTC Transformer with LDC

The assumption of uniform load distribution indicates that the active and reactive power flow drop linearly with distance  $d$  from the substation as described in Chapter 2 and repeated here for convenience, i.e.,

$$P_d = P_s \left(1 - \frac{d}{l}\right), \quad Q_d = Q_s \left(1 - \frac{d}{l}\right) \quad (3-1)$$

where  $P_s$  and  $Q_s$  are the MW and MVAR flow at the substation end of the feeder, and  $l$  is the total length of the line as illustrated in Fig. 3-2. The per-unit (pu) value of the total voltage drop across the feeder can be approximated by [27]

$$VD_d = \frac{l(RP_s + XQ_s)}{2V_b^2} \quad (3-2)$$

where  $V_b$  is the nominal line-to-line voltage (kV), and  $R$  and  $X$  represent the feeder equivalent resistance and inductive reactance in Ohms per mile.

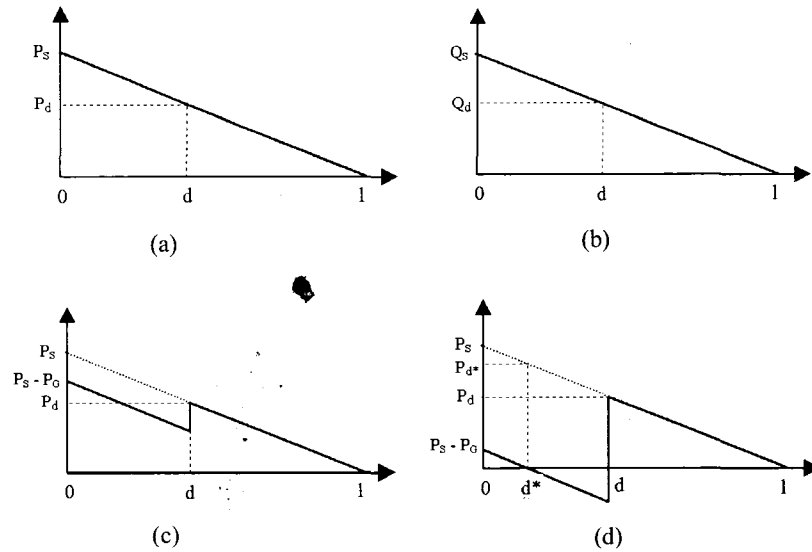


Fig. 3-2: Active and Reactive Power Profile along Feeder without and with DG at Distance  $d$  from Substation.

The above voltage drop will be altered when a DG is installed on the feeder, and its deviation depends on both the DG size and location. Let  $P_G$  be the real power produced by a DG that is installed at some distance  $d$  from the substation. The modified expressions of the voltage drop for Case I (when  $P_G < P_d$ ), and Case II (when  $P_G > P_d$ ) are derived next.

### 3.1.A. Case I: $P_G < P_d$

When  $P_G < P_d$ , the voltage drop can be decomposed in two components as illustrated in Fig. 3-2(c): The voltage drop between the substation and DG location, and voltage drop between the DG location and feeder end.

Voltage drop between 0 and  $d$ :

$$VD_{0-d} = d \frac{R(P_d - P_G) + XQ_d}{V_b^2} + \frac{d}{2} \frac{R(P_d - P_G) + X(Q_s - Q_d)}{V_b^2} \quad (3-3-1)$$

Voltage drop between  $d$  and  $l$ :

$$VD_{d-l} = \frac{(l-d)RP_d + XQ_d}{2V_b^2} \quad (3-3-2)$$

The total voltage drop across the feeder is then approximated by

$$VD = VD_{0-d} + VD_{d-l} \approx \frac{l(RP_s + XQ_s) - 2dRP_G}{2V_b^2} \quad (3-3)$$

### 3.1.B. Case II: $P_G > P_d$

This case is illustrated in Fig. 3-2(d) where power flow reversal exists. This causes the so-called “zero point” denoted by  $d^*$  in the graph, where active power flows “uphill” towards the substation to the right of the zero point, and “downhill” in a conventional way to the left of the zero point. It is clear from Fig. 3-2(d) that the zero point is computed by

$$d^* = \left(1 - \frac{P_G}{P_S}\right)l \quad (3-4-1)$$

In here, the voltage drop is computed across each of the three line segments as follows:

Voltage drop between 0 and  $d^*$ :

$$VD_{0-d^*} = \frac{d^* R(P_S - P_G) + X(Q_S + Q_d^*)}{2V_b^2} \quad (3-4-2)$$

Voltage drop between  $d^*$  and  $d$ :

$$VD_{d^*-d} = \frac{(d - d^*) R(P_d - P_G) + X(Q_d + Q_d^*)}{2V_b^2} \quad (3-4-3)$$

where

$$Q_d^* = Q_S \left(1 - \frac{d^*}{l}\right) \quad (3-4-4)$$

Voltage drop between  $d$  and  $l$ :

$$VD_{d-l} = \frac{(l - d) RP_d + XQ_d}{2V_b^2} \quad (3-4-5)$$

The total voltage drop across the feeder can be obtained by summing the three voltage drops above:

$$\begin{aligned} VD &= VD_{0-d^*} + VD_{d^*-d} + VD_{d-l} \\ &\approx \frac{dR(XQ_d^* - P_G) + (RP_S + XQ_S) \left\{ l + d \left( \frac{d^*}{l} - 1 \right) \right\}}{2V_b^2} \end{aligned} \quad (3-4)$$

### 3.2 Critical DG Size and Location

Note that the voltage drop above in Eqn. (3-4) is both a linear function of the DG size  $P_G$  (i.e.,  $VD = \alpha P_G + \beta$ ) as well as location  $d$  (i.e.,  $VD = \lambda d + \sigma$ ). Hence one can easily

determine either a critical DG size of fixed location, or a critical location of a fixed DG size, that can result in maximum allowable voltage drop  $VD$ . The maximum allowable  $VD$  depends on the magnitude of the voltage  $V_S$  set by the LTC with LDC at the substation end:

$$VD_{\max} = V_S - 0.95. \quad (3-5-1)$$

The magnitude of  $V_S$  at the substation can be approximated by a linear function of the power flow at the substation end:

$$V_S = 1 + 0.05 \frac{P_S - P_G}{P_S} \quad (3-5)$$

Hence, for a given DG of size  $P_G$ , its minimum distance from the substation that does result in an under-voltage at the feeder end is computed by

$$d_{\min} = \frac{1}{\lambda} (V_S - \sigma - 0.95) \quad (3-6)$$

Likewise, the maximum DG size located at a fixed location  $d$  that results in an acceptable voltage at the feeder end is approximated by

$$P_{G-\max} = \frac{P_S(0.1 - \beta)}{\alpha + 0.05} \quad (3-7)$$

### 3.3. Summary

This chapter illustrates the possibility of experiencing under-voltages towards the end of a distribution feeder (whose voltage is regulated by and LTC transformer with LDC) when a DG of significant size is connected close to the substation end. In such a situation, the DG “fools” the tap controls by making the feeder load appear to have a lighter load, thus reducing the substation voltage to a value lower than necessary. On the other hand, maintaining the substation voltage at the highest permissible value by

disabling the LDC controls may result in over-voltages when a sufficiently large DG unit is installed towards the feeder end. As a consequence, coordination between distributed generator output and LTC transformer tap controls is necessary to avoid voltage regulation problems.

## CHAPTER 4

### THE IMPACT OF DG ON VOLTAGE REGULATION IN FEEDERS WITH SWITCHED CAPACITORS

Loading on typical distribution feeders can vary significantly throughout the day, and proper reactive power compensation is achieved through the use of a combination of fixed and switched capacitor banks [28]-[30]. Meanwhile, the widespread use of Distributed Generation (DG) is predicted to expand rapidly and will constitute a significant portion of new power generation in the future. While DG is known to reduce power loss and to release system capacity, power system operations may be adversely impacted if certain minimum standards for control and interconnection are not met [32].

As pointed out earlier, a DG of sufficient size may cause an over-voltage condition if a thorough analysis of the distribution feeder is not conducted. This condition can be worsened by some control types of switched capacitors as they come on line. Unfortunately, very limited technical articles concerning the revision of switched capacitor control settings prior to installing distributed generation on the same feeder are available [13].

This chapter intends to broaden this discussion in an effort to provide some tools for distribution engineers to address this potentially serious problem prior to installing distributed resources. It focuses on the voltage regulation of a feeder that is equipped with fixed and switched capacitors, and to which a DG is about to be connected to. First,

some assumptions to simplify the analysis are presented. This is followed by a brief review of the various types of capacitor controls and DG characteristics in terms of generated power. Then approximate voltage profile along the feeder with and without DG and switched capacitors is calculated from the daily load curve. The impact of DG and capacitor switching scenarios on the voltage curve is analyzed. The problem will be illustrated through a numerical example in Chapter 5.

#### 4.1 Assumption of Scenario of Distribution System with DG

Voltage along typical distribution feeders in general is regulated by a combination of switched capacitors and substation load tap changing transformer that is typically equipped with a line drop compensator (LDC). Longer feeders may also require a line voltage regulator. Coordinating these devices, in addition the presence of DG is a monumental task to deal with. In order to simplify the analysis, the following assumptions are made:

- A. *The voltage is held constant at the substation by the LTC transformer (i.e., the fixed voltage point maintained by the LDC is at the substation).* In other words, the LDC is disabled due to numerous problems including potential serious consequences of switched capacitors beyond the regulating point [30].
- B. *The feeder has no line voltage regulator.* DG and voltage regulators tend not to mix. It is known that when a DG is applied downstream of a voltage regulator, it will confuse the regulator into setting a voltage lower than is required for adequate service [12]. This will either limit the DG operating range or will require complicated DG-regulator coordination algorithms [16].

- C. *The DG consists of one sufficiently large unit.* The impact of an individual residential scale DG unit (less than 10 kW) on the primary feeder is negligible. An aggregate capacity of many small units deployed will have similar effect of a large unit.
- D. *Available data includes hourly load demand on the feeder, switched capacitor placement and method of control, feeder data and Distributed Generator characteristics.* Such data are needed for the analysis that follows.

#### 4.2 Capacitor Control and DG Type

The response of switched capacitors to some DG coming on line depends on the type of capacitor controls, and the resulting voltage deviation also depends on the real as well as reactive powers injected by the DG. Hence it is worth reviewing capacitor control methods and types of DG in use.

##### 4.2.A. *Types of Capacitor Controls*

There are several types of switching controls for capacitor banks in common use including time, temperature, voltage, current, kVAR, radio and intelligent controls. Each method has its own advantages and disadvantages, and many utilities use a combination of these methods.

- ◆ Time control is the simplest and least expensive method to switch capacitors. In the past, time control suffered from numerous problems, but now it is more sophisticated with battery backup and a number of layers of control logic programmability to account for weekends, holidays, and different seasons.

- ◆ Temperature control is another very inexpensive and simple method that is targeted to areas where reactive power loading varies directly with temperature, such as the air conditioning load. It is most attractive in situations where loads have a good degree of predictability, with little or no abnormality.
- ◆ Voltage control involves monitoring the line voltage, i.e., switching ON when the voltage dips below a certain preset value, and conversely switching OFF when the voltage rises above another preset value. This method is often used to supplement other control methods in emergency situations.
- ◆ Current control involves monitoring the line current, and it works well if the power factor of the load is fairly constant. Current control cannot differentiate between low and high power factor.
- ◆ VAR control monitors the real-time VAR loading and compensates reactive power as needed (i.e., has the ability to differentiate between high and low power factor).
- ◆ Intelligent control uses multiple inputs in the capacitor switching algorithm to mitigate shortcomings that single input controls might have. A simple example includes time control supplemented by voltage control. In here, the primary control (i.e., temperature) controls the capacitor switching unless an emergency threshold is reached on the secondary control, a point at which the secondary control (i.e., voltage) takes over switching of the capacitor bank.

- ◆ Unlike the above schemes where control is automated locally by a measure of some variable, radio control is simply an extension of the SCADA system onto distribution feeders. This allows operators to switch ON and OFF capacitors as needed, any utilities are integrating radio control into distribution automation for system optimization.

#### 4.2.B. Distributed Generation Type

DG technologies include photovoltaic panels, wind turbines, fuel cells, small turbine packages; Stirling-engine based generators and internal combustion engine generators. Inverter-based generators are often designed to operate at unity power factor. Conventional synchronous machines can both supply and absorb reactive power, but induction generators used in wind and Stirling engine systems can only operate at a lagging power factor (i.e., absorb reactive power while generating real power).

One complicated issue with DG is that those based on renewable resources (e.g., solar and wind) are not dispatchable as they come on line only when the resource is available. Furthermore, most DG units are expected to be owned and operated by customers rather than the electric utility, and customer needs do not often match with utility needs.

#### 4.3 Approximate Voltage Profile with DG and Capacitor Control

Radial distribution feeders are represented by the concentrated load model shown in Fig. 4-1(a) where  $P_m(t)$  and  $Q_m(t)$  represent the load active and reactive power consumption at node  $m$  ( $m=1,2, \dots,n$ ) at time  $t$ . For simplicity, only one switched capacitor is shown at node  $i$  upstream of the distributed generator to be installed at node  $j$ . Note that permanently fixed capacitors are not shown since they can be lumped as part of the load.

The effects of capacitor and DG switching on the daily feeder power demand are illustrated in Fig. 4-1(b) where the DG is shown to operate at unity power factor. Approximate power flow along the feeder and node voltages can be calculated by simple analytical expressions that depend on whether the switched capacitors and DGs are turned ON or OFF. These expressions for different DG/switched capacitor combinations follow.

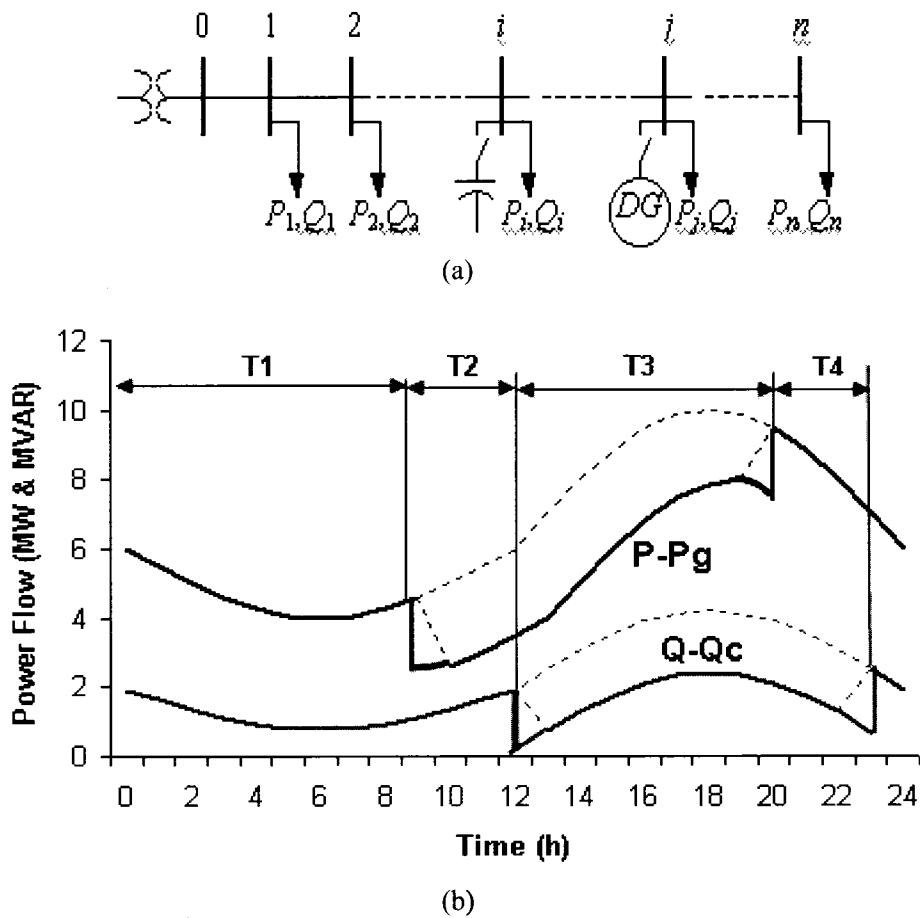


Fig. 4-1: (a) Feeder with DG and Switched Capacitors;  
(b) Daily Power Curves with Switched Capacitors and DG.

#### 4.3.A. With both Capacitor and DG Switched OFF

Prior to the capacitor and DG switching at light load (during period  $T_l$  in Fig. 4-1(b)), the real and reactive power flow in line segment  $(k-1,k)$  can be approximated by the sum of the loads connected at nodes  $k$  through  $n$ ,

$$P_{k-1,k}(t) = \sum_{m=k}^n P_m(t) \quad (4-1)$$

$$Q_{k-1,k}(t) = \sum_{m=k}^n Q_m(t) \quad (4-2)$$

The voltage profile along the feeder is computed recursively starting with  $V_o(t)$  fixed at 1.05 pu at the substation bus, where  $(R_{k-1,k}, X_{k-1,k})$  represent the resistance and inductive reactance of line segment  $(k-1,k)$ , and  $VD_k(t)$  is the voltage drop across line segment  $(k-1,k)$ . This voltage drop is approximated by Chapter 2,

$$V_k(t) = \frac{1}{2} \left\{ V_{k-1}(t) + \left[ V_{k-1}^2(t) - 4VD_k^d(t) \right]^{1/2} \right\} \quad (4-3)$$

$$VD_k^d(t) = \frac{R_{k-1,k}P_{k-1,k}(t) + X_{k-1,k}Q_{k-1,k}(t)}{V_b^2} \quad (4-4)$$

where  $V_b$  is the base voltage.

#### 4.3.B. With Capacitor Switched ON and DG Switched OFF

As the load increases to a point where the capacitor controls is activated, the active power flow is nearly unchanged and is still computed by Eqn. (4-1), while the reactive power is reduced by  $Q_C$  upstream of the capacitor location, i.e., for  $k > i$  the reactive power flow is computed by Eqn. (4-2), and for  $k \leq i$ ,

$$Q_{k-1,k}(t) = -Q_C + \sum_{m=k}^n Q_m(t) \quad (4-5)$$

#### 4.3.C. With DG Switched ON and Capacitor Switched OFF

Unlike the application of shunt capacitors, many types of distributed generators are able to deliver both active power  $P_G$  and reactive power  $Q_G$  into the system. However, if the installed DG operates at a leading power factor as in the case of an induction generator, its reactive component  $Q_G$  is negative and will have opposite effect. With a DG switched ON at node  $j$ , the power flow in line segment  $(k-1,k)$  is computed by Eqns. (4-1)-(4-2) for  $k > j$ , and by Eqns. (4-6)-(4-7) below for  $k \leq j$ . The plus and minus signs in Eqn. (4-7) correspond to generator operating at a lagging and leading power factor, respectively.

$$P_{k-1,k}(t) = -P_G(t) + \sum_{m=k}^n P_m(t) \quad (4-6)$$

$$Q_{k-1,k}(t) = \pm Q_G(t) + \sum_{m=k}^n Q_m(t) \quad (4-7)$$

#### 4.3.D. With both Capacitor and DG Switched ON

When both switched capacitor and DG are turned ON (i.e, during time period  $T_3$  in Fig. 4-1(b)), the power flow in feeder segment  $(k-1,k)$  is calculated by Eqns. (4-1)-(4-2) for  $k > j$ , by Eqns. (4-6)-(4-7) for  $i < k \leq j$ , and by Eqn. (4-6) and

$$Q_{k-1,k}(t) = -Q_C \pm Q_G(t) + \sum_{m=k}^n Q_m(t) \quad (4-8)$$

for  $k \leq i$ .

The above analysis can also be extended to multiple DG units and multiple switched capacitor banks without much difficulty, but the calculations can quickly become elaborate as the number of possible switching combinations rises exponentially.

#### 4.4 Impact of DG and Switched Capacitor on Voltage Regulation

Both fixed and switched capacitors are placed on distribution feeders after a detailed analysis of the load characteristics. Switching of capacitors is selected to achieve numerous benefits such as minimizing reactive power flow from the substation transformer, reducing power and energy loss, and maintaining the voltage within acceptable limits. Introducing significant distributed resources on such feeders will reduce the power demand. Depending of the type of controls used, existing capacitor switching may lead to significant over-voltages if not revised to accommodate the distributed generator units.

To illustrate the above concern, consider the simple case in Fig. 4-1(a) where one DG is installed downstream of one switched capacitor. Prior to presence of the DG unit, it was determined that best system operation is achieved by having the capacitor controls switch ON at 12:00 PM and OFF at 11:00PM, as shown in the Fig. 4-1(b). Such operation assures that the voltage along the feeder does not violate the upper and lower limits. Now the DG is introduced and is scheduled to generate  $P_G$  MW at unity power factor from 9:00AM to 8:00PM. How will the capacitor controls react to this change? The answer depends on the type of controls used:

- ◆ With time or temperature controls, the capacitor switches ON and OFF as before, but because the power demand is reduced by that produced by the DG, an over-voltage at and near the capacitor node may occur temporarily for few hours.
- ◆ With current and voltage controls, capacitor switching will be delayed and the ON period will be shortened since lower power demand often results in lower

current flow and in higher voltage. This leads to a rise in kVARh demand from the transmission system.

- ◆ With VAR controls, the capacitor switches ON and OFF as before unless the DG operates at a power factor other than unity. This case may result in over-voltages at the vicinity of the capacitor bank location.
- ◆ With intelligent controls having the voltage signal as the supplementary controls, the unit switches ON then it will likely switch OFF as it senses higher voltages. This ON/OFF switching may be repeated numerous times and may lead to failure of the switch mechanism and annoying capacitor switching transients.
- ◆ With SCADA controls, a new optimum capacitor switching schedule is extracted from the modified system and no problems are expected.

#### 4.5. Summary

This chapter calls for the attention to revise the switched capacitor control settings before installing distributed generation units on distribution feeders. Ignoring such a study may lead to the potential problem of over-voltages that occur after switched capacitors come on line. The over-voltage depends on numerous factors including DG size, type of capacitor controls, and feeder load characteristics.

## CHAPTER 5

### NUMERICAL EXAMPLE OF THE IMPACT OF DG ON VOLTAGE REGULATION

Chapters 2, 3 and 4 analyzed the impact of DG on voltage regulation along distribution feeders both with and without LTC transformer and switched capacitor banks. To illustrate the analyses presented earlier, an actual circuit with slightly modified parameters is studied in this chapter. The circuit consists of a 30 MVA 138/12.47 kV LTC transformer with 11% impedance that supplies a 4-mile long distribution feeder (394MCM cable with rated capacity of 600A). The resistance and inductive reactance (GMD = 5') of the line are 0.28  $\Omega$ /mi and 0.64  $\Omega$ /mi, respectively. A schematic of this feeder is shown in Fig. 5.1, and its section lengths and installed peak load at each of the 11 nodes are listed in Table 5.1 below. Note that the total peak load is  $(P_0, Q_0) = (10 \text{ MW}, 5 \text{ MVAR})$ .

In the first case study, i.e., Case I, the LTC of the substation transformer is assumed to adjust the secondary voltage to 1.05 pu at all time, and switched capacitors are ignored. Then, in Case II, the LTC of the substation transformer is assumed to adjust the secondary voltage to 1.05 at peak load, and down to 1 at no load in a linear fashion, and switched capacitors are also ignored. Finally, in Case III, the LTC of the substation transformer is assumed to adjust the secondary voltage to 1.05 pu at all time, and two fixed capacitors and two switched capacitors are installed to compensate the reactive

power.

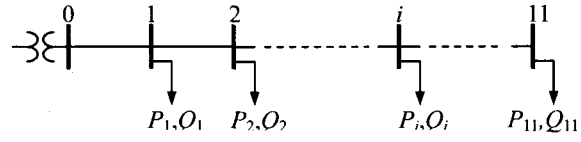


Fig 5-1: Radial Distribution Circuit.

Table 5-1: Feeder and Load Data

$i$	$d_{i-1,i}$ (mi)	$P_i$ (MW)	$Q_i$ (MVAR)
1	0.80	2.1	1.3
2	0.45	1.4	0.8
3	0.30	1.0	0.6
4	0.25	0.5	0.1
5	0.20	0.8	0.2
6	0.25	0.6	0.3
7	0.55	0.9	0.5
8	0.25	1.3	0.6
9	0.30	0.3	0.1
10	0.40	0.5	0.2
11	0.25	0.6	0.3

### 5.1 Case I: Impact of DG on Voltage Profile on Feeder with Fixed Substation Voltage

A placement of a DG unit at node 5 is to be investigated. The effect of the DG placement on the voltage profile is investigated by two methods: (a) Assuming the load is uniformly distributed and using Eqns. (2-6)-(2-9); (b) Using the concentrated loads method and using Eqns. (2-13)-(2-15). The results of both methods are compared to the computer simulation solution obtained by a power flow program, EasyPower, which uses circuit nodal analysis to compute the voltage, current and power flow of the power system.

Fig. 5-2 shows four voltage profile curves obtained by assuming a uniformly distributed load. The green curve is the voltage profile without DG. The blue, black and red curves correspond to the voltage profile with DG operating at 8 MW and 100% power factor, 91% power factor lag, and 80% power factor lag, respectively. When the DG is set to generate 8 MW, the maximum reactive power it can generate without exceeding the upper voltage limit of 1.05 is 3.5 MVAR, corresponding to PF = 91% lag.

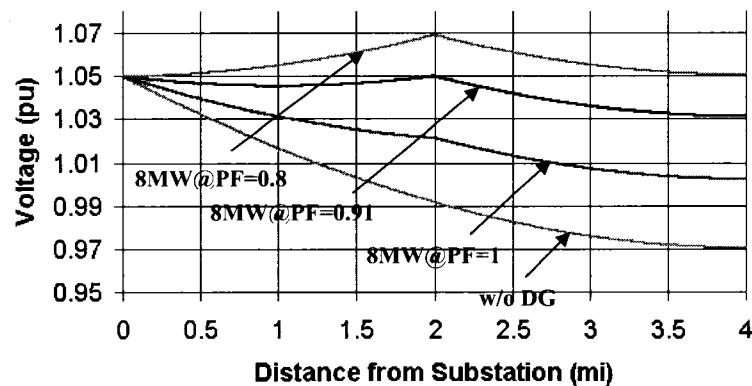


Fig. 5-2: Voltage Profile without & with DG Supplying 8MW at Different PF (with Uniform Loads)

Eqn. (2-10) indicates that the maximum power that can be generated by the DG without violating voltage limits decreases linearly with distance from the substation. Fig. 5-3 shows three curves of such maximum power as a function of distance  $d$  when the DG is set to operate at 95%, 90% and 80% power factor (lag). If the DG is set to operate at a leading power factor (i.e., absorb reactive power), then the voltage rise caused by  $P_G$  will be offset by the additional voltage drop caused by,  $Q_G$ . In this case, the maximum DG power will be significantly higher.

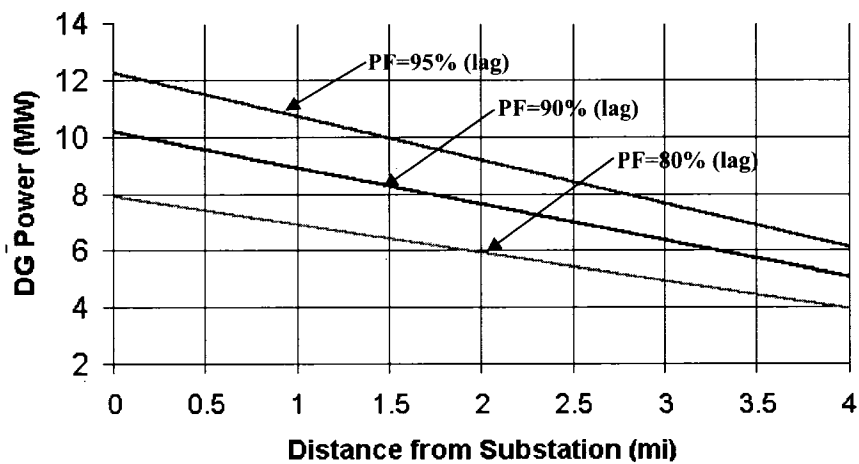


Fig. 5-3: Maximum DG Real Power Output as Function of Distance from Substation

Fig. 5-4 shows the resulting voltage profile when using the concentrated load method that is expected to be more accurate than the uniformly distributed load method for this circuit under study. These curves are piecewise linear since the load is concentrated only at the nodes shown and closely resemble the smooth curves in Fig. 5-2. In addition, slight differences can be noted at only few nodes.

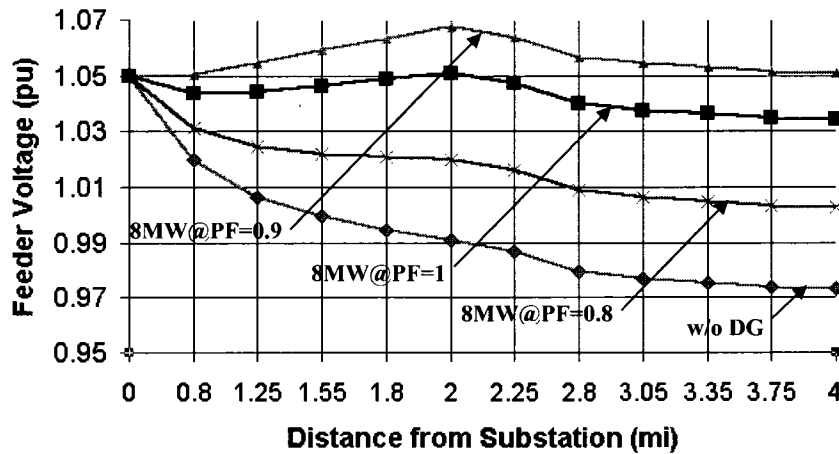


Fig. 5-4: Voltage Profile without & with DG Supplying 8MW at Different PF (with Concentrated Loads).

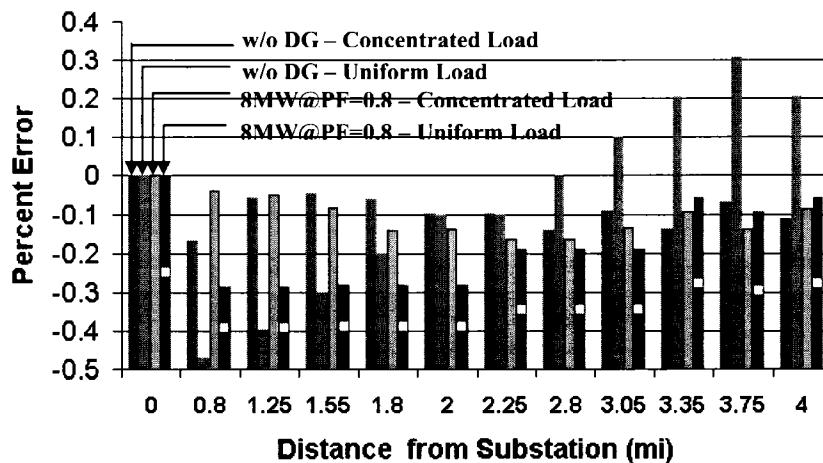


Fig. 5-5: Percent Errors of Node Voltages Obtained Uniform Loads and Concentrated Loads Methods w/o and with DG at Node 5.

To check the accuracy of the results obtained by both analytical methods, the node voltage values are compared to the exact ones obtained by a load flow computer program. Fig.5-5 shows these errors for the two extreme voltage profile curves (the one without DG, and the one with DG supplying 8 MW @ 80% power factor lag). It is noted that

although the concentrated load method is more accurate than the uniformly distributed load method, the largest error is well within 0.5%. Consequently, the simple method where the load is assumed to be uniformly distributed along the feeder is probably more than adequate for similar feeders.

## 5.2 Case II - Impact of DG on Voltage Regulation with LTC Transformer Action

To check the accuracy of the approximate expressions derived in Chapter 3, the same example circuit with uniformly distributed load model is revisited in this section. According to the analysis in Chapter 2, the error between the uniformly distributed load model and concentrated load model is within 1%, hence only the uniform load is considered here. The LTC transformer is further assumed to adjust the secondary voltage to 1.05 pu at peak load, and down to 1 pu at no load in a linear fashion.

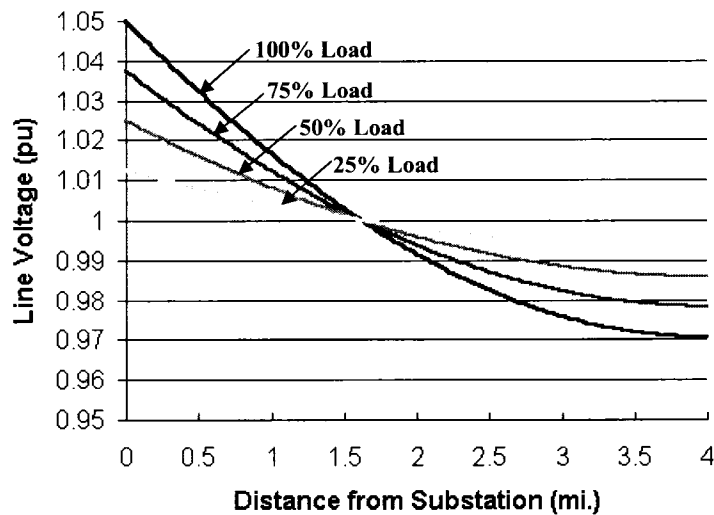


Fig. 5-6: Feeder Voltage Profile at Different Load Levels Prior to DG Installation.

Prior to DG installation, the voltage profile along the feeder is shown in Fig. 5-6 for four load levels, i.e., 100%, 75%, 50%, and 25% of peak load. The LDC controls adjusts the LTC transformer tap such that the feeder voltage at 1.6 mi from the substation is maintained at the nominal value of 1 pu. The largest voltage drop of 8% occurs during peak load (as indicated by the black-colored curve). The voltage drop calculated by Eqn. (3-2) during peak load is 7.7%. Hence, the approximations made are sufficiently accurate.

Fig. 5-7 shows the new voltage profile after installing a 5 MW distributed generator (or 50% DG penetration during peak load) at different locations along the feeder. The voltage profile curve prior to DG installation is also shown in the Fig. 5-7 for reference purposes. When this particular DG is installed at the end of the feeder, it tends to raise the voltage from 0.972 pu to 0.984 pu, thus providing voltage support. On the other hand, when it is moved close to the substation, it causes the last mile of the feeder to operate at a voltage below 0.95 pu. This situation is often referred to as “the fooling of LTC by DG” since it confuses the LTC by setting a voltage lower than is required to maintain adequate service. The minimum distance  $d_{min}$  from the substation that a 5 MW DG unit will result in acceptable voltage throughout the feeder is estimated to be 0.6 mi by Eqn. (6). The green curve in Fig. 5-7 represents the corresponding voltage profile, and is in agreement since the voltage barely reaches the minimum allowed value at the feeder end.

Fig. 5-8 shows the voltage profile for different DG sizes installed at a fixed point located 1 mi from the substation during peak load. The maximum DG size at this particular location that will not result in under-voltage at the feeder end is estimated by Eqn. (3-7) to be 6.4 MW. The corresponding voltage curve (pink color) verifies that such a limit is sufficiently accurate.

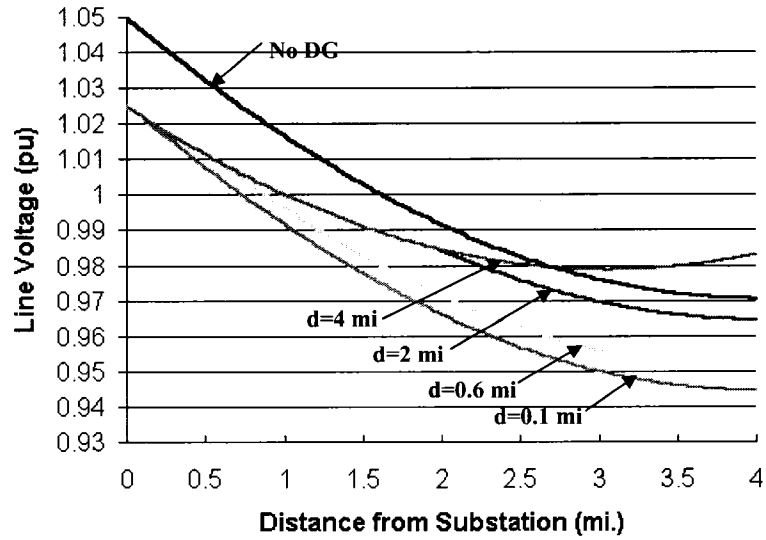


Fig. 5-7: Voltage Profile with 5 MW DG Installed at Different Locations during Peak Load.

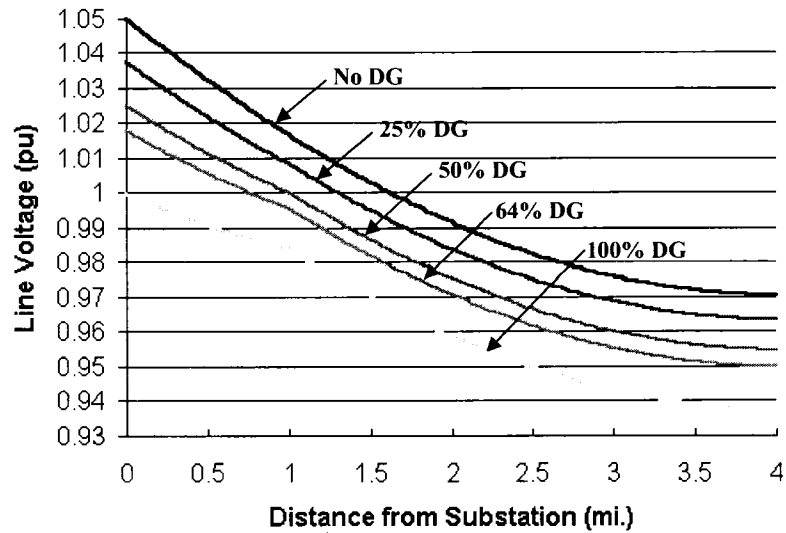


Fig. 5-8: Voltage Profile for Different DG Sizes Installed at 1 mi from Substation during Peak Load

### 5.3 Case III - Impact of DG on Voltage Regulation with Switched Capacitors

To illustrate the analysis in Chapter 4, the same example circuit with concentrated load model is used in this section. The LTC for the substation transformer is assumed to adjust the secondary voltage to 1.05 pu at all time. In terms of VAR compensation, the feeder is assumed to have 2 fixed capacitor banks (one at node 5 and one at node 6) and two switched banks at node 4. Each capacitor bank is rated at 1,200 kVAR. Both banks are temperature controlled (the first is set to turn ON at 90° F and the second at 100° F).

Fig. 5-9 shows the active and reactive power profile over a 24 hour period during a hot summer day as well as the temperature variation. The reactive power curve clearly shows the capacitor switching times (the first capacitor turned ON when the temperature reached near 90 degrees at 9 AM and the second capacitor turned ON when the temperature reached near 100 degrees around 11:30 AM). Note that the second capacitor switched OFF around 7 PM, while the first capacitor remained ON since the temperature stayed above the preset value.

Fig. 5-10 displays the calculated voltage profile along the feeder immediately before and after the first and second switched capacitor banks came on line (at 9:00 AM and 11:30 AM, respectively). Note that the voltage is at the upper limit of 1.05 pu at busses 4 – 6 right after the first bank came ON.

Fig. 5-11 shows how the voltage of some of the feeder nodes, namely, nodes 4, 7 and 11, vary during the three capacitor switching times and at some other times. Clearly node 4 is on the verge of exceeding the upper limit while node 11 at the feeder end is of least concern.

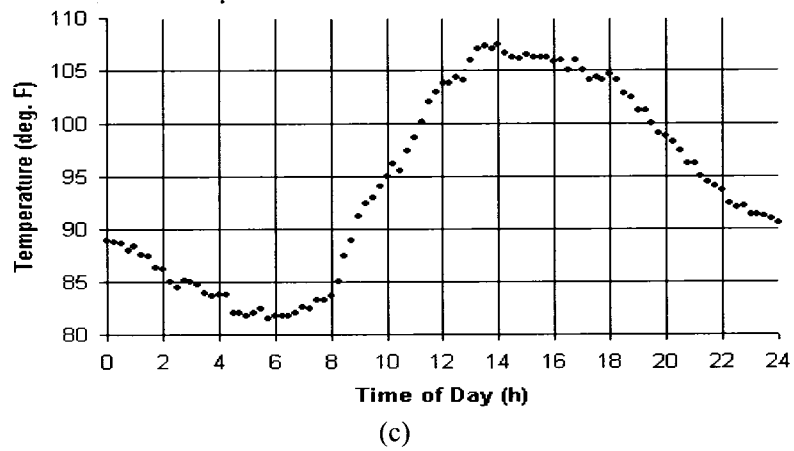
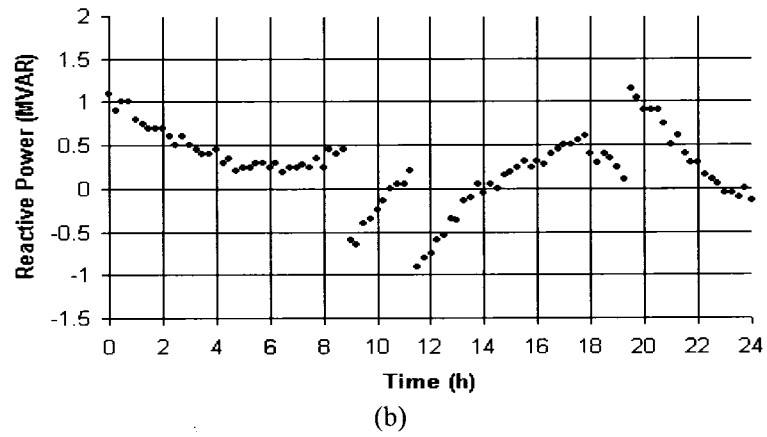
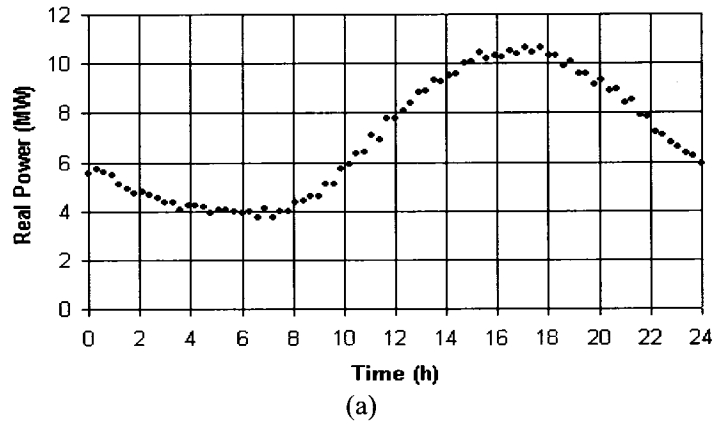


Fig. 5-9: (a) Feeder Real Power; (b) Feeder Reactive Power; (c) Ambient Temperature during Peak Demand.

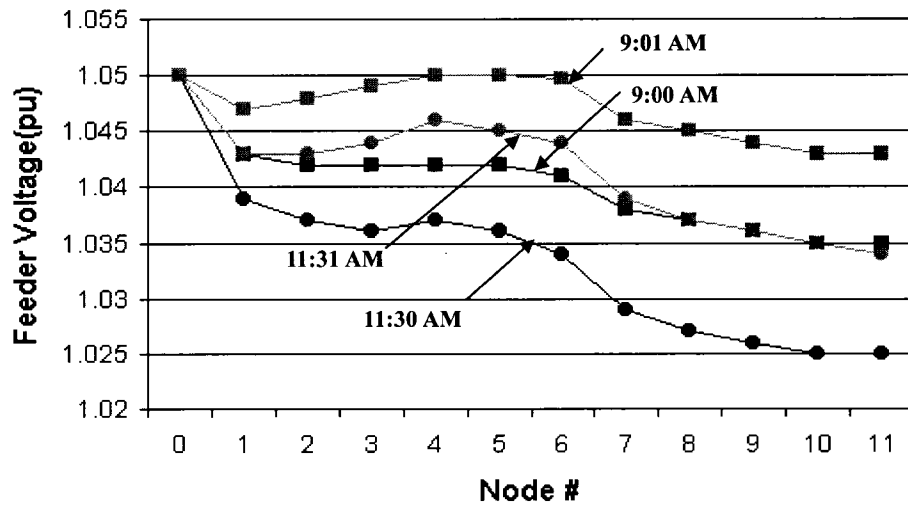


Fig. 5-10: Voltage Profile before and after Capacitor Switching (w/o DG).

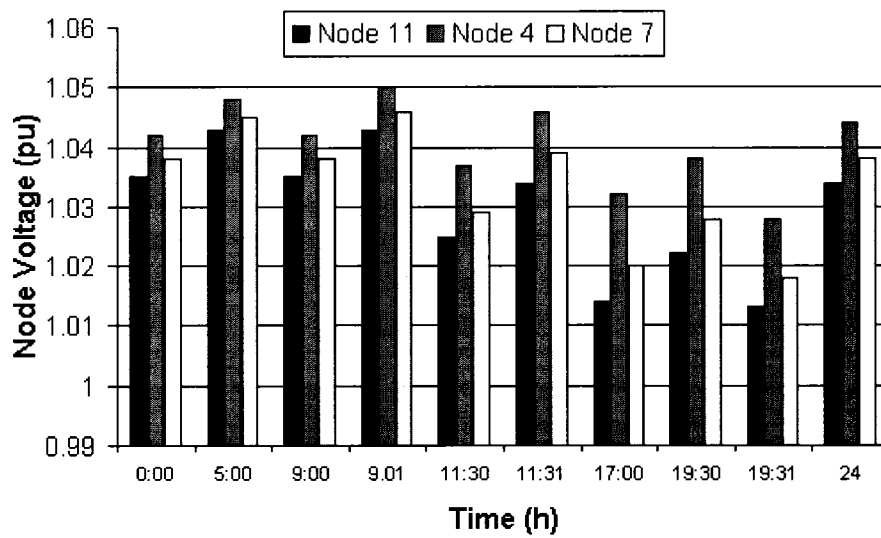


Fig. 5-11: Time Variation of Some Feeder Node Voltages (w/o DG)

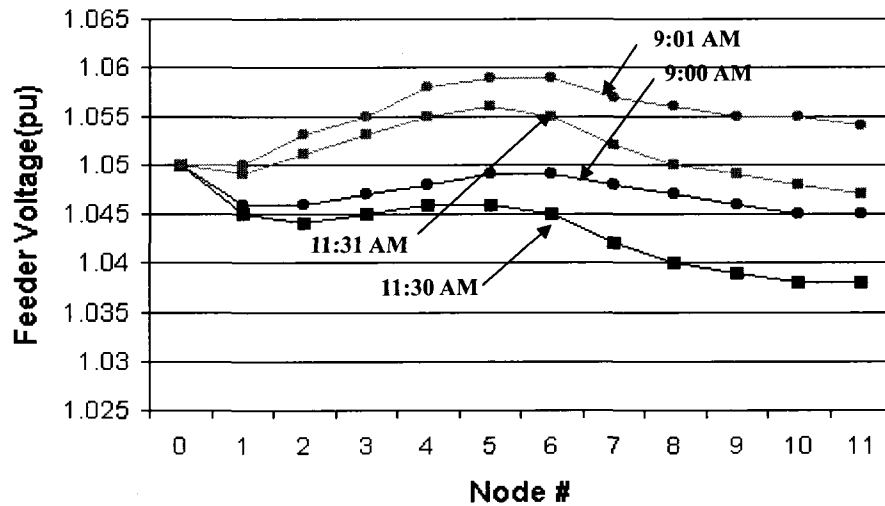


Fig. 5-12: Voltage Profile before and after Capacitor Switching (with 2 MW DG at Node 7)

Now it is of interest to install a 2 MW distributed generator at node 7. Without modifying switched capacitor control settings, one can immediately conclude from Fig. 5-10 and Fig. 5-11 that such installation will lead to over-voltages during some periods of time after capacitor switching. This is illustrated in Fig. 5-12 that displays the modified node voltages just before and after the switching of the two capacitor banks. Note that the voltage profile prior to capacitor switching is satisfactory. But all feeder nodes and more than half of the nodes experience an over-voltage after the first and second capacitor banks are switched ON, respectively.

#### 5.4 Summary

The above numerical example illustrates the problem of voltage regulation when a DG unit is introduced into a radial distribution system, when taking LTC transformer with LDC controls and switched capacitors into account. The example verifies the accuracy of the analytical results concluded in Chapters 2-4, and clearly demonstrates the

potential under- or over-voltages that may occur. It can be concluded that the negative impact of DG would happen if the old voltage regulation scheme of the feeder is not modified after DG penetration. The many factors that could affect the occurrence and severity of the problems include the size(s) of the DG unit(s), the location(s) of DG(s), the feeder and load characteristics, and the type(s) of the old voltage regulation scheme(s). In short, before a DG unit is introduced into a distribution system, the voltage profile should be examined carefully in order not to allow it go out of range.

## CHAPTER 6

### ISLANDING STUDIES OF INVERTER-BASED DG

One major category of DG devices is inverter-based distributed generation, namely, systems that require power conversion by means of power electronic converters. These include photovoltaics (PV) systems, fuel cells system, battery storage systems, and micro-turbines. One of the obstacles for the widespread application of such DG systems in power networks is concern over islanding, i.e., when the disconnected part of the power network is sustained by the connected PV systems for a significant period of time. Islanding must be avoided for several reasons including, the creation of a hazard for utility line workers by touching a line that should be otherwise de-energized, lack of control over voltage and frequency in the islanding area, and interference with restoration of normal service [22]-[24].

In response to the above concern, inverter manufacturers now market the so-called “non-islanding” inverters that are expected to meet current interconnection standards. According to IEEE Std. 1547 [32], these non-islanding inverters are expected to disconnect within 0.16 seconds, or 10 cycles, if the voltage drops below 50% or rises above 120% of its nominal value. The same maximum clearing time applies if the frequency drops below 59.3 Hz or rises above 60.5 Hz (based a 60 Hz nominal value). If the voltage drops to a value between 50% and 88%, or rises to a value between 110% and 120% of the nominal value, the allowed clearing time is expanded to 2 seconds, and 1

second, respectively.

Standard protection of grid-connected inverter-based DG systems consists of four relays: over-voltage relay, under-voltage relay, over-frequency relay, and under-frequency relay. These relays will prevent islanding under most circumstances, as they disconnect the PV system from the utility in the event that the magnitude or frequency of the inverter's terminal voltage falls outside specified limits. However, if the local load closely matches the power produced by the inverter, the resulting deviations in voltage and/or frequency after a power outage may be too small to detect, i.e., fall within the non-detection zone. In this case, additional passive or active schemes are required to minimize the probability of an island to occur [33]-[37].

This chapter first reviews the standard protection against islanding based on the detection of voltage and/or frequency deviations. The magnitudes of these deviations are derived for constant impedance loads in terms of active and reactive power mismatch coefficients. This is followed by the review of some of the most popular additional passive as well as active schemes that have been proposed to further reduce the possibility of islanding. Then a MATLAB model is designed and constructed to build up a platform for the simulation of islanding phenomenon and design of anti-islanding techniques for the inverter-based DG.

### 6.1 Review of Anti-islanding Techniques

To simplify the analysis, a PV system is proposed as a representative example of all inverter-based DG systems to be discussed in this chapter. It has been reported that grid-tied PV systems normally operate at or near unity power factor, and this makes sense from an economic point of view, which also applies to almost all inverter-based DG

systems. To settle such uncertainty, several local systems have been tested and they were found to operate between 98% and 99% power factor leading. So while the above statement can be considered correct, nonetheless, PV inverters do generate a small amount of reactive power that cannot be ignored in an island condition.

Consider Fig. 6-1 where a PV system is tied to the local grid under the presence of a local load. For simplicity, the load is considered of constant impedance type (i.e., a parallel R-L circuit) that consumes  $P_L$  watts and  $Q_L$  vars. The active and reactive powers generated by the PV system are denoted by  $P_D$  and  $Q_D$ , respectively. The utility system is shown to supply  $P_S$  in watts and  $Q_S$  in vars. These powers are related as follows:

$$P_D + P_S = P_L \quad (6-1)$$

$$Q_D + Q_S = Q_L \quad (6-2)$$

Assume the load is linear RLC type of load. And let the ratio of  $P_S/P_D = \alpha$ , and  $Q_S/Q_D = \beta$ . Then the above equations can be rewritten as

$$P_D(1 + \alpha) = V^2 / R \quad (6-3)$$

$$Q_D(1 + \beta) = V^2 / \omega L \quad (6-4)$$

where  $V$  and  $\omega$  represent the voltage at the interconnection point and system angular frequency, respectively.

When the utility disconnects, both  $P_S$  and  $Q_S$  go to zero and the voltage and frequency ( $V, \omega$ ) will settle to new values ( $V', \omega'$ ). These new values are related to the original ones the following equations:

$$V' = \frac{1}{\sqrt{1 + \alpha}} V \quad (6-5)$$

$$\omega' = \frac{1 + \beta}{1 + \alpha} \omega \quad (6-6)$$

The above expressions show that the deviations in voltage and frequency depend on the level of power mismatch as well as direction of  $P_S$  and  $Q_S$ . Possible combinations are listed below:

Case A:  $P_S > 0$  and  $Q_S > 0$ : The voltage decreases. The frequency depends on the values of  $\alpha$  and  $\beta$ . If  $\alpha = \beta$ , then the frequency remains the same. If  $\alpha > \beta$ , the frequency decreases. If  $\alpha < \beta$ , the frequency increases. In particular, for those DG systems having utility power factor output, which means always  $P_D = 0$ , thus  $\beta$  goes to positive infinity, the frequency will increase to positive infinity finally.

Case B:  $P_S > 0$  and  $Q_S < 0$ : Both the voltage and frequency decrease.

Case C:  $P_S < 0$  and  $Q_S > 0$ : Both the voltage and frequency increase.

Case D:  $P_S < 0$  and  $Q_S < 0$ : The voltage increases. The frequency depends on the values of  $\alpha$  and  $\beta$ . If  $\alpha = \beta$ , then the frequency remains the same. If  $\alpha > \beta$ , the frequency increases. If  $\alpha < \beta$ , the frequency decreases. Again for those DG systems having utility power factor output, the frequency will decrease to 0 finally.

Case E:  $P_S = 0$  and  $Q_S \neq 0$ : The voltage remains constant, while the frequency changes (i.e., decreases if  $Q_S < 0$  or increases if  $Q_S > 0$ ).

Case F:  $P_S \neq 0$  and  $Q_S = 0$ : The frequency remains constant, while the voltages change (i.e., increase if  $P_S < 0$  or decrease if  $P_S > 0$ ).

Case G:  $P_S = 0$  and  $Q_S = 0$ : Both the voltage and frequency remain constant.

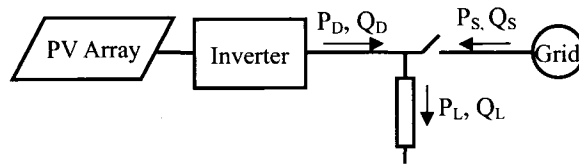


Fig. 6-1: Grid-connected PV System with Local Load

Note that one of the over-voltage, under-voltage, over-frequency, or under-frequency relays will sense the voltage and/or frequency change in Cases A through F, hence preventing islanding. In Case G where the PV power production matches the load power requirement, however, none of these relays will operate since no change occurs in voltage and frequency. In reality,  $P_S$  and  $Q_S$  do not have to be exactly zero for this to occur because the magnitude and frequency of the utility voltage are expected to deviate slightly from nominal values. Therefore, the thresholds for the four relays cannot be set arbitrarily small or else the PV system will be subject to nuisance trips. This limitation leads to the formation of the so-called “Non Detection Zone” (NDZ) [39]. It is therefore important that PV systems incorporate ways to prevent islanding in the case where  $P_S$  and  $Q_S$  are very small.

Many islanding detection techniques and anti-islanding techniques have proposed in the past years. These can be grouped into two categories: passive methods and active methods [38]. The most common ones are briefly described below.

*6.1.A. Passive Methods:*

- a) Under/over voltage and under/over frequency detection, where the inverter monitors the voltage and frequency shift. This method is universally adapted to all DG systems and set standard by IEEE or other standard organizations. This

method results in a NDZ whose size depends on the standard adopted by the DG system and the control types and control scheme of the inverter.

- b) *Voltage Phase jump detection*, where the phase between the inverter's terminal voltage and its output current is monitored for sudden jumps.
- c) *Voltage harmonic monitoring*, where the inverter monitors change in the voltage total harmonic distortion and shuts down if this parameter exceeds some threshold [40].

#### 6.1.B. Active Methods:

- a) *Impedance measurement*, where the inverter monitors the change in the inverter output circuit impedance, which occurs when the low impedance distribution network is disconnected. To accomplish this method, several different techniques may be employed [42], like power variation, signal injection and load insertion [43].
- b) *Frequency and phase shift techniques*, where a positive feedback is applied to the control loops that control inverter phase, frequency, or reactive power so that the inverter frequency will shift rapidly to the under/over frequency detection threshold when the grid is not present to maintain the frequency.
- c) *Voltage shift techniques*, where a positive feedback is applied to the current or active power control loop so that the inverter terminal voltage will shift rapidly to the under/over voltage detection threshold when the grid is not present to maintain the voltage.

#### 6.2 Construction of MATLAB Model for the Inverter-Based DG

Several design models of DG systems can be found in the literature [45]-[50].

However, some of models are constructed in system level for system operation and planning, while some are constructed in equipment level for the details of specific types of DG units [45]-[47]. A general model in the circuit level to illustrate and anti-islanding technique appears to be lacking. This section presents a general model for and inverter-based DG system which can be used for the demonstration of islanding detection. The selection of MATLAB Simulink platform is made due to its strong ability to design the control scheme in detail and customize components in a flexible manner.

The circuit representing a grid-tied PV system, as shown in Fig. 6-2, is modeled in this section. Yet this model can be easily used to simulate other types of inverter-based DG systems like fuel cells and wind turbines. The research work focuses on the behavior of the DG immediately after the loss of the grid. A constant DC voltage source is adapted for the source after regulation from the PV panels. This DC source is inverted to 3-phase AC through the inverter and the LC filter, and then connected to the local load through a relay, followed by grid connection through the line breaker, which controls the time of the disconnection.

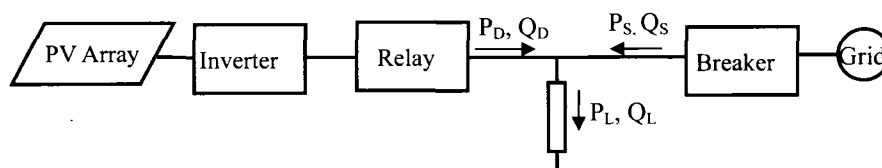


Fig. 6-2: Block Diagram of the Grid-tied PV System

There are three major sections in the grid-tied PV system. One is the PV section, including the PV Array and the inverter, another is the local load section, and the last one is the grid section. Further, there are two connectors to joint the PV section to the local

load section, and the local load section to the grid section.

- ◆ For the first connector, a relay is needed to accomplish the control function required by IEEE Std. 929-2000 [22], to disconnect the PV from the outside load and grid in case of over-voltage, under-voltage, over-frequency, and under-frequency. Thus, the relay control scheme is designed as shown in Fig. 6-3.
- ◆ For the second connector, only a line breaker is needed to simulate the disconnection from the grid, whose scheme is designed as shown in Fig. 6-4. The control signal to the line breaker is time-setting. When the time reaches the preset timeline, the breaker will act to disconnect grid from the other parts of the system. Since it is suggested to cancel the re-closer function in the DG-connected system, the line breaker is not designed to re-close after a few cycles.

The relay control-signal generator in Fig. 6-3(b) compares the RMS value and the frequency of the voltage at the output port to the setting up-limits and down-limits of the voltage and the frequency. If any limit is exceeded, the logic gates will give a rising signal to act the relay to disconnect the PV to the outside network. However, in case the relay act during the some temporary incidents such as spikes or sags, time delay is employed to ensure the limits broken is not temporary but lasting for a long time. Thus, if a limit is violated last more than 10 cycles, which is about 0.167s, the generator will consider the network is violating the voltage or frequency limits, which usually means some accident happens in the network. At this point, the generator will supply the relay a control signal to shut off the connection of the PV system to the outside network.

With the implementation of the two connectors in place, the grid is implemented by a constant three-phase voltage AC source, the load is implemented by a balanced three-phase RLC load, and the PV section uses a constant DC voltage source to simulate the regulated voltage from PV panel arrays. The DC voltage source is inverted to three-phase AC source through a PWM inverter and an LC filter. The most difficult and important part is the design of the PWM inverter.

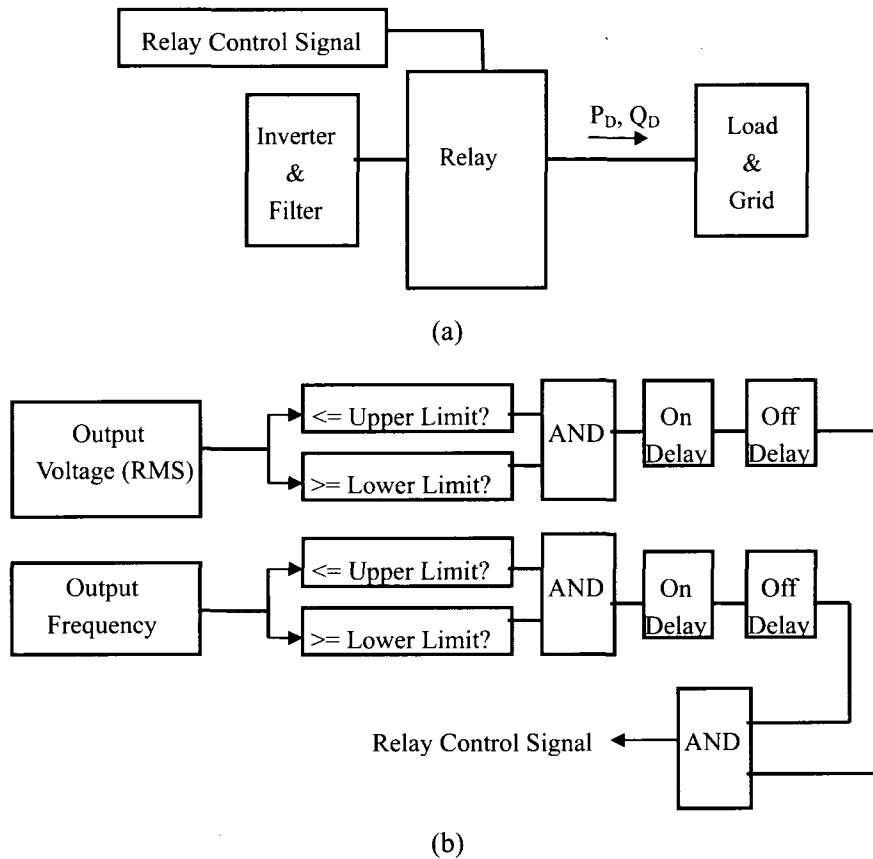


Fig. 6-3: (a) Relay Control Scheme and (b) Relay Control Signal Generator

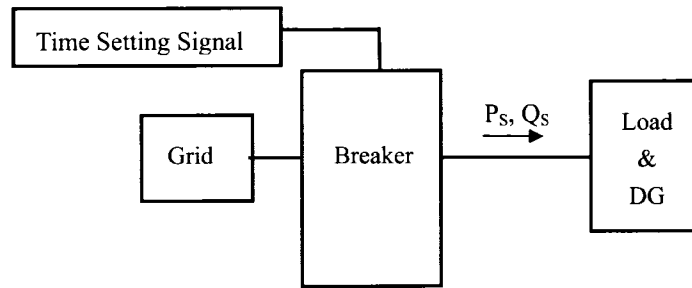


Fig. 6-4: Breaker Control Scheme

The PWM inverter used by most PV systems on the market needs to meet the following requirements:

- ◆ The output voltage of the PV system must be coherent to the outside voltage, which means the same or almost same magnitude and frequency.
- ◆ The output power of the PV system must be constant.
- ◆ The output power of the PV system must have a near unify power factor.
- ◆ In case of the change of the output voltage, the output of the PV system must change with it as quick as possible.

These requirements need to be implemented in the PWM control, which is by no means a simple task. There are two major PWM techniques in the power industry applications, the voltage-mode PWM control and the current-mode PWM control. The two control types have their own advantages and disadvantages.

Initially, the voltage-mode PWM control is applied to the design of the inverter for its characteristics. To meet the above requirements of the inverter, the PWM control have the following features:

- ◆ The reference voltage magnitude must be proportional to the outside one.
- ◆ The reference voltage frequency must be same as the outside one.

- ◆ The reference voltage phase angle must be tuned to make the output real power to the setting value and the output reactive power to through zero.
- ◆ In case of change in the output voltage, the reference voltage magnitude and phase angle must change with it as quick as possible.



Fig. 6-5: Circuit to Determine the Control Equations for Voltage Mode PWM

When the impedance of the relay is ignored, and only the fundamental component of the voltage at the output port of the inverter  $V_{PV}$  is considered, the simplified circuit can be concluded like Fig. 6-5 to determine the control equations of the PWM control. The node m is on the output port of the relay, which connects to the load and the outside grid. The measured voltage at node m is  $V_m@0$ . The node n is on the output port of the inverter, where the fundamental component of the voltage is  $V_{PV}@\delta$ . The LC filter is between nodes m and n. Since the capacitance has no effect on the real power flow on branch n-m, only the inductance reactance  $X_L$  is taken into consideration.

Further, it is known that for the voltage-mode PWM controller if the reference voltage in PWM is set as  $V_{ref}@\delta$ , then it can be found that  $V_{PV}@\delta = KV_{ref}@\delta$ . Hence, the constant power output requirement means that  $P_D$  is keep constant, and  $Q_D$  keep almost zero at steady-state condition. From Fig. 6-5, the control equations can be concluded to determine the reference voltage based on the measured voltage at node m to make the output real power the setting value and reactive power roughly zero, i.e.,

$$P_D = \frac{V_{PV} V_m}{X_L} \cos \delta = \frac{KV_{ref} V_m}{X_L} \cos \delta \quad (6-7)$$

$$Q_D = \frac{V_{PV}^2}{X_L} - \frac{V_{PV} V_m}{X_L} \sin \delta = \frac{K^2 V_{ref}^2}{X_L} - \frac{KV_{ref} V_m}{X_L} \sin \delta \quad (6-8)$$

When the phase angle  $\delta$  is small,  $\cos \delta \approx 1$  and  $\sin \delta \approx \delta$ , the above equations simplify to:

$$P_D = \frac{KV_{ref} V_m}{X_L} \quad (6-9)$$

$$Q_D = \frac{K^2 V_{ref}^2}{X_L} - \frac{KV_{ref} V_m}{X_L} \delta = 0 \quad (6-10)$$

which yield:

$$V_{ref} = \frac{K' P_D}{V_m} \quad (6-11)$$

$$\delta = \frac{KV_{ref}}{V_m} \quad (6-12)$$

So the conclusion can be drawn that the reference voltage magnitude is determined by setting output real power and the measured voltage magnitude; while the phase angle is determined by the reference voltage magnitude and the measured voltage magnitude. It is impossible to decouple the two control loops of the voltage magnitude and phase angle.

Thus, the control scheme must be designed in two steps:

- ◆ First, adjust the voltage magnitude to the wanted value;
- ◆ Second, adjust the phase angle to the wanted value.

However, because of the approximation in the equations and the computation errors in the design, both parameters can't be directly set to the wanted values, but to be controlled in negative feedback loops to make the control of both parameters accurate and stable. In other words, the control scheme must be designed as a two-level nested

feedback controller loop to meet the requirements of the PWM controller, in which the inner loop controls the magnitude control and the out loop controls the phase angle.

The two PI controllers must be designed very carefully to let the out loop changes slower than the inner loop, yet not too slow to unable to catch up with the change on node m. But it turns out to be very hard to coordinate the adjustment of two PI controllers' parameters to make the two-level loop work smoothly on most cases, and the response time of the out loop for the phase angle control is always not fast enough. This problem becomes worse when the outside voltage changes in a significant manner. This is because the measurements of the outside voltage's magnitude and phase angle are based on the average value not the instantaneous value, so that the correct measurements can't be feedback to the sensor in real-time but after few cycles, which makes the time delay problem even worse. In many cases, the phase angle can't be converged to the new value after 30 cycles and more. And in some cases, when the outside voltage changes rapidly, the phase angle can never converge to the correct steady-state value. For the difficulties of coordinating the adjustment of the inner loop and outer loop parameters and solving the time delay problem, the voltage mode PWM control scheme is abandoned and the current-mode PWM control scheme is the alternative method to turn to.

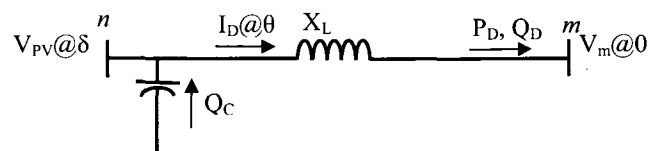


Fig. 6-6: Circuit to Determine the Control Equations for Current-Mode PWM

If the current mode PWM control scheme is adopted based on Fig. 6-5, and the

capacitance is small enough so that  $Q_C$  can be neglected, it is known that the output current should satisfy the following relation:  $I_D @ \theta = KV_{ref} @ \theta$ . The control equations are derived from the circuit in Fig. 6-6:

$$P_D = V_m I_D \cos \theta = KV_m V_{ref} \cos \theta \quad (6-13)$$

$$Q_D = -V_m I_D \sin \theta = -KV_m V_{ref} \sin \theta \quad (6-14)$$

Again when the phase angle  $\delta$  is small, the equations change to:

$$P_D = KV_m V_{ref} \quad (6-15)$$

$$Q_D = -KV_m V_{ref} \theta = 0 \quad (6-16)$$

And they can be represented in other forms:

$$V_{ref} = \frac{K' P_D}{V_m} \quad (6-17)$$

$$\theta = 0 \quad (6-18)$$

Eqn. 6-18 is valid because  $V_m$  and  $V_{ref}$  will never be zero in the considered scenarios. Then,  $\theta$  must be zero for the case of perfect unity power factor. Thus, the two control loops for current magnitude and current phase angle are decoupled in the current-mode PWM controller. Even after taking into consideration  $Q_C$ , the phase angle is only determined by  $Q_C$ . The reason is that at under steady-state condition, the Eqns. (6-19) and (6-20) must be satisfied:

$$Q_D = Q_C - KV_m V_{ref} \theta = Q_C - P_D \theta = 0 \quad (6-19)$$

$$\theta = \frac{Q_C}{P_D} \quad (6-20)$$

In most cases,  $Q_C$  is very small compared to  $P_D$ . Then  $\theta$  is very small. If the output reactive power is not required to be near zero, no measurement of  $Q_C$  is required, and

only the use of a PI controller to adjust  $\theta$  (to let the output reactive power fluctuate around zero) is needed. So it is found that that two feedback loops for current magnitude control and phase angle control are decoupled in current mode PWM scheme, so that both loops can be designed separately.

Unlike the design of the voltage mode PWM control scheme, the decoupled feedback loops design reduces the difficulty to coordinate two PI controllers to zero, and reduces the transition time delay greatly. The PI controllers in both feedback loops can be optimized separately to make the response as fast as possible. And because  $V_m$  is always near 1 and  $\theta$  is always near 0, the initial values are very easy to set independently with the specific scenarios and are always very close to the target values, so that the design not only reduces the responding time even more but enhances the robustness of the control system.

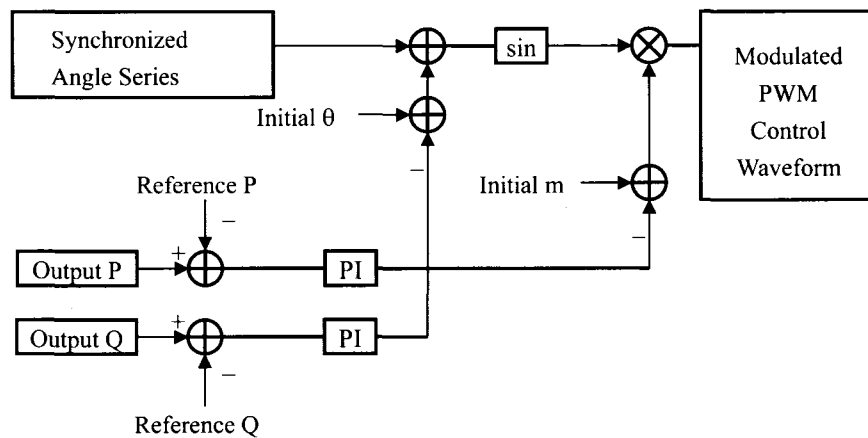


Fig. 6-7: PWM Control Waveform Generator

From the analysis of the control scheme design, the whole control diagram of the current mode PWM control waveform generator can be designed as shown in Fig. 6-7. In

here, the input of the synchronized sinusoidal waveform is replaced by the synchronized angle series, which can simplify the computation when the angle is changing. Moreover, the output real and reactive power are measured and compared to the reference real and reactive power. The error is feedback to the control factor of the phase angle  $\theta$  and modulation index  $m$  through the PI controllers respectively. And lastly, the modulated  $\theta$  is added to the synchronized angle series and the modulated  $m$  is multiplied to the sinusoidal waveform respectively. Then the control waveform for the current mode PWM controller is generated.

From the above analysis for each section in the grid-tied PV system, the model is built for each section according to their characteristics. And when those sections are put together, a MATLAB model of the grid-tied PV system is ready for the simulation of the behaviors of the DG, relay, load voltage and current, etc. And the Appendix II gives the complete set of the MATLAB model of the system.

## CHAPTER 7

### ISLANDING SIMULATION AND FIELD TEST RESULTS

Based on the MATLAB model described in Chapter 6, the different scenarios are simulated to verify the conclusions on circuit behavior and islanding drawn in Chapter 6. There are 6 cases simulated in this chapter. The first 4 cases are when the PV system's output real and reactive power mis-matches the load requirements. In those cases, the terminal voltage and frequency will shift from the values when the grid is connected. And the 5<sup>th</sup> case is when the PV system's output real and reactive power matches the load requirements perfectly. In this case, the islanding will happen if only over/under voltage and over/under frequency are detected. The last case applies an anti-islanding technique to the circuit in the 5<sup>th</sup> case. And the simulation shows the feasibility of the anti-islanding technique.

Other than the computer simulation, the field islanding tests are demonstrated on two local grid-tied PV installations. The experiment records illustrate how the PV system response to the grid outage in presence of the local loads.

#### 7.1 Islanding Simulation

Several cases are conducted simulation on the MATLAB model described in Chapter 6. All these simulation cases verify the conclusions on circuit behavior and islanding drawn in Chapter 6. Some typical cases are presented below.

7.1.A. Case A:  $P_S > 0$ ,  $Q_S > 0$

The grid-tied PV system is constructed as described in Chapter 6. In the model, the load is set as  $P_L = 8\text{kW}$  and  $Q_L = 2\text{kVar}$  at nominal voltage and frequency. And the PV panel's output is set as  $P_D = 7\text{kW}$ , and  $Q_D = 0$ . Thus, we can easily know that in steady state,  $P_S = 1\text{kW}$  and  $Q_S = 2\text{kVar}$ .

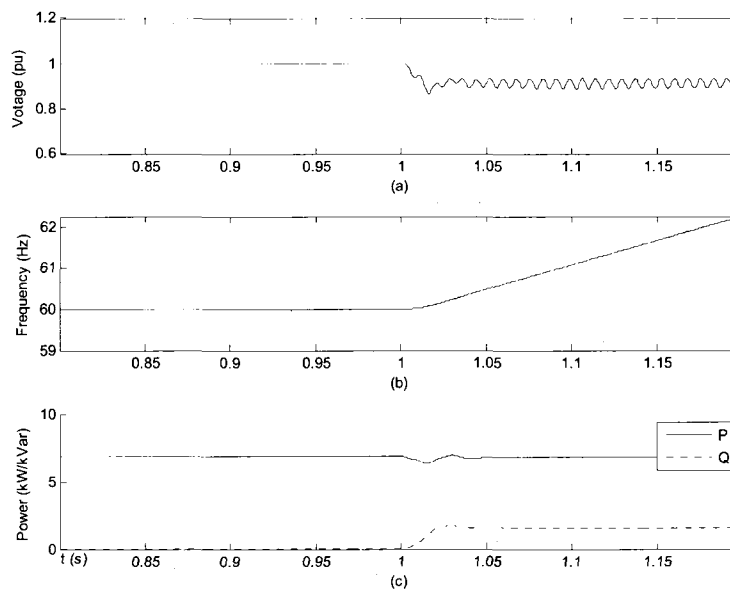


Fig. 7-1: Inverter Terminal Voltage, Frequency & Output Real and Reactive Power (with Relay Set to Non-function)

The simulation set the scenario as that the grid is disconnected at 1s. With the relay set to non-function, which means the PV panel is always connected to the load. The output voltage (RMS value), frequency and real and reactive power is shown in Fig. 7-1. Compared to the analysis in Chapter 6, the dynamics of voltage and frequency are the same as the conclusion in Chapter 6. Note that the frequency increases to infinity slowly

because the output reactive power of PV system should be zero at steady-state.

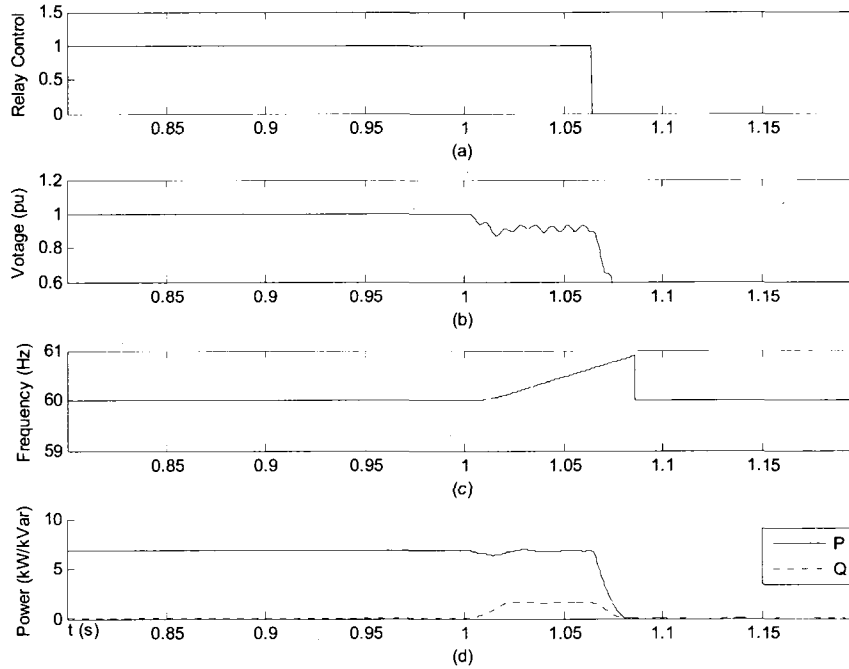


Fig. 7-2: Inverter Terminal Voltage, Frequency & Output Real and Reactive Power and Relay Control Signal (with Relay Set to Function)

When the relay is set to function, the simulation results are shown in Fig. 7-2. The relay control signal shows the relay respond at about 0.07s, which is about 4-5 cycles, after the disconnection of the grid happens.

#### 7.1.B. Case B: $P_S > 0$ , $Q_S < 0$

The grid-tied PV system is constructed as described in Chapter 6. In the model, the load is set as  $P_L = 8$  kW and  $Q_L = -2$  kVar at nominal voltage and frequency. And the PV panel's output is set as  $P_D = 7$  kW, and  $Q_D = 0$ . Thus, we can easily know that in steady state,  $P_S = 1$  kW and  $Q_S = -2$  kVar.

The simulation in Fig. 7-3 shows that in this case the output voltage and frequency both drop after the disconnection of the grid, which is consistent with the analysis in Chapter 6.

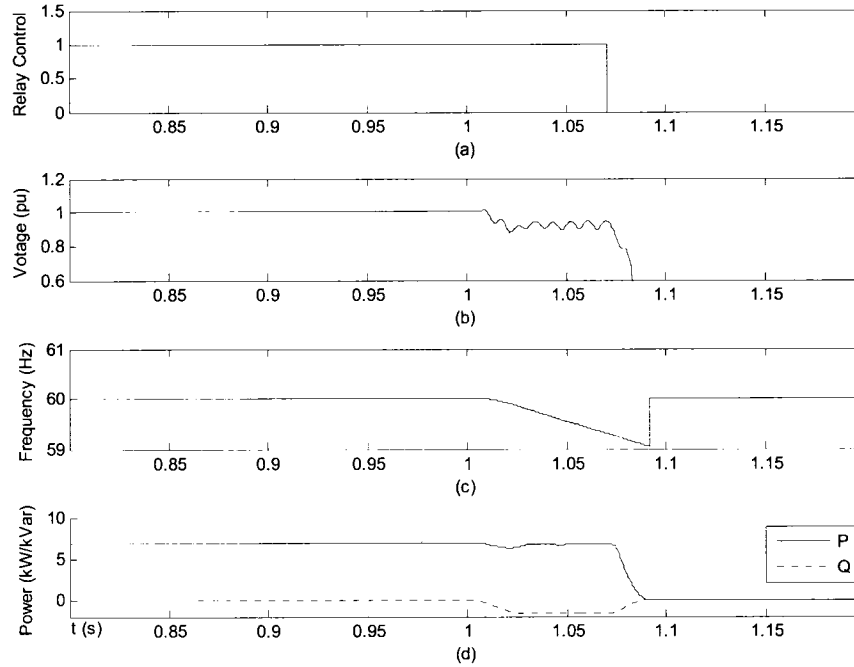


Fig. 7-3: Inverter Terminal Voltage, Frequency & Output Real and Reactive Power and Relay Control Signal (with Relay Set to Function)

### 7.1.C. Case C: $P_S < 0$ , $Q_S > 0$

The grid-tied PV system is constructed as Fig. 6-1. In the model, the load is set as  $P_L=8\text{kW}$  and  $Q_L=2\text{kVar}$  at nominal voltage and frequency. And the PV panel's output is set as  $P_D=9\text{kW}$ , and  $Q_D=0$ . Thus, we can easily know that in steady state,  $P_S=-1\text{kW}$  and  $Q_S=2\text{kVar}$ .

The simulation in Fig. 7-4 shows that in this case the output voltage and frequency

both increases after the disconnection of the grid, which is consistent with the analysis in Chapter 6.

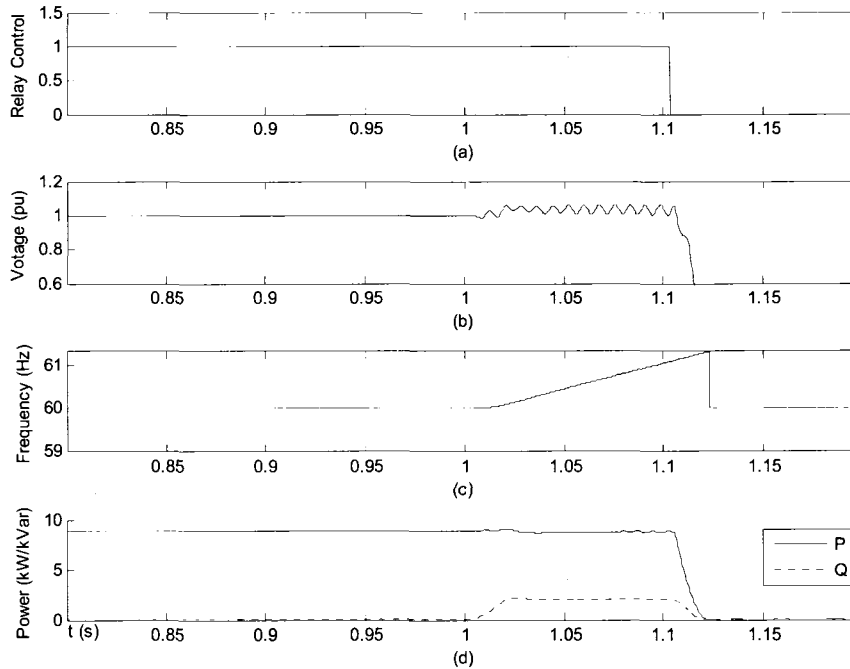


Fig. 7-4: Inverter Terminal Voltage, Frequency & Output Real and Reactive Power and Relay Control Signal (with Relay Set to Function)

7.1.D. Case D:  $P_S < 0$ ,  $Q_S < 0$

The grid-tied PV system is constructed as described in Chapter 6. In the model, the load is set as  $P_L=8\text{kW}$  and  $Q_L=-2\text{kVar}$  at nominal voltage and frequency. And the PV panel's output is set as  $P_D=9\text{kW}$ , and  $Q_D=0$ . Thus, we can easily know that in steady state,  $P_S=-1\text{kW}$  and  $Q_S=-2\text{kVar}$ .

The simulation in Fig. 7-5 shows that in this case the output voltage increases and frequency drops after the disconnection of the grid, which is consistent with the analysis

in Chapter 6.

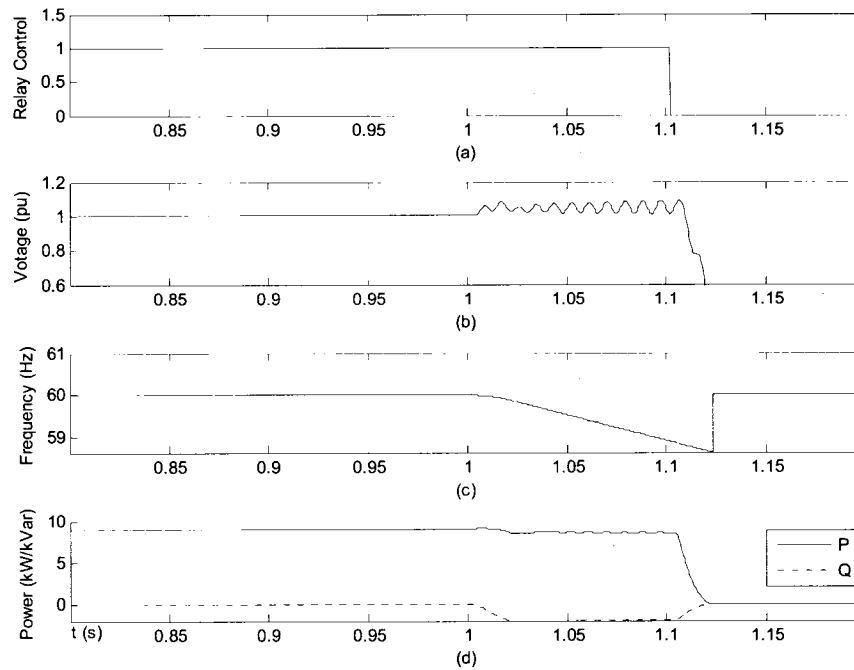


Fig. 7-5: Inverter Terminal Voltage, Frequency & Output Real and Reactive Power and Relay Control Signal (with Relay Set to Function)

7.1.E. Case E:  $P_S=0$ ,  $Q_S=0$

The grid-tied PV system is constructed as described in Chapter 6. In the model, the load is set as  $P_L=8\text{kW}$  and  $Q_L=0$  at nominal voltage and frequency. And the PV panel's output is set as  $P_D=8\text{kW}$ , and  $Q_D=0$ . Thus, we can easily know that in steady state,  $P_S=0$  and  $Q_S=-2\text{kVar}$ . According to the analysis in Chapter 5, this will result in no or little difference on output voltage and frequency. And in such case, the islanding phenomenon appears.

The simulation in Fig. 7-6 shows that the output voltage and frequency both are

almost the same as those before the disconnection of the grid, which is consistent with the analysis in Chapter 6. And the relay doesn't act because it couldn't sensor any difference between before and after the disconnection of the grid. And the simulation shows the islanding phenomenon successfully.

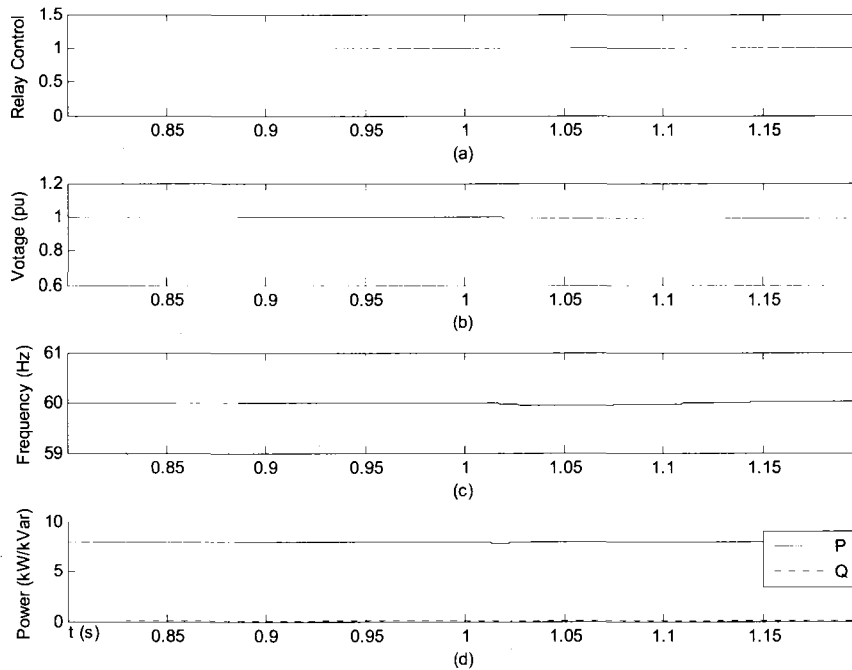


Fig. 7-6: Inverter Terminal Voltage, Frequency & Output Real and Reactive Power and Relay Control Signal (with Relay Set to Function)

7.1.F. Case F:  $P_S=0$ ,  $Q_S=0$ , with a periodically connected capacitor.

According to the above simulation cases, the occurrence of islanding is demonstrated. After a series of cases selected and-tested, we roughly get the Non Detection Zone (NDZ) of the DG model built in Chapter 6, which is about a square of the mismatch reactive power ( $Q_S$ ) from -350Var to 350Var and the mismatch real power ( $P_S$ ) from -580W to

580W with the nominal output power of the inverter is 8kW in unity power factor. This means when the load consumption reactive power in the range of  $\pm 4.4\%$  error and real power in the range of  $\pm 7.3\%$  of the inverter nominal output power, the islanding phenomenon will occur.

Here a novel simple method of anti-islanding technique is presented and tested. A small capacitor of 800VAR capacity is installed in shunt on the feeder just out of the inverter terminal. Thus, the NDZ will shift to the range of mismatch reactive power ( $Q_s$ ) from 450Var to 1150Var (which is named NDZ-II), compared to the case without capacitor installed of the range of mismatch reactive power ( $Q_s$ ) from -350Var to 350Var (which is named NDZ-I). If we add a switch between the capacitor and the feeder, and control it to put the capacitor in operation periodically, the NDZ then will shift also from NDZ-I to NDZ-II periodically. In this way, with the area out of NDZ-I and NDZ-II still detectable, these two non detection zones become two slow detection zones. The reason is the worst case for the load in the two non detection zones is that the grid is disconnected when the NDZ is in function. When this happens, the disconnection will stay undetected until the NDZ shifts to the other in the longest time of half switching period of the capacitor. As long as the relay is fast enough to detect and act in the other period, the NDZ will be eliminated and only be detected slowly in some cases.

Fig. 7-7 shows the case that the capacitor of 800Var installed with a switching period of 0.167s, which is 10 cycles. Compared to Case E, the islanding case, it now can be detected. However, compared to other non-islanding cases, it can be found the voltage and frequency stayed almost unchanged when the grid disconnected at 1s. Only after half of the capacitor switching period of about 0.9s, the voltage and frequency shift and then

the relay act when the frequency out of range for 5 cycles. This simulation result verifies the feasibility of this anti-islanding scheme.

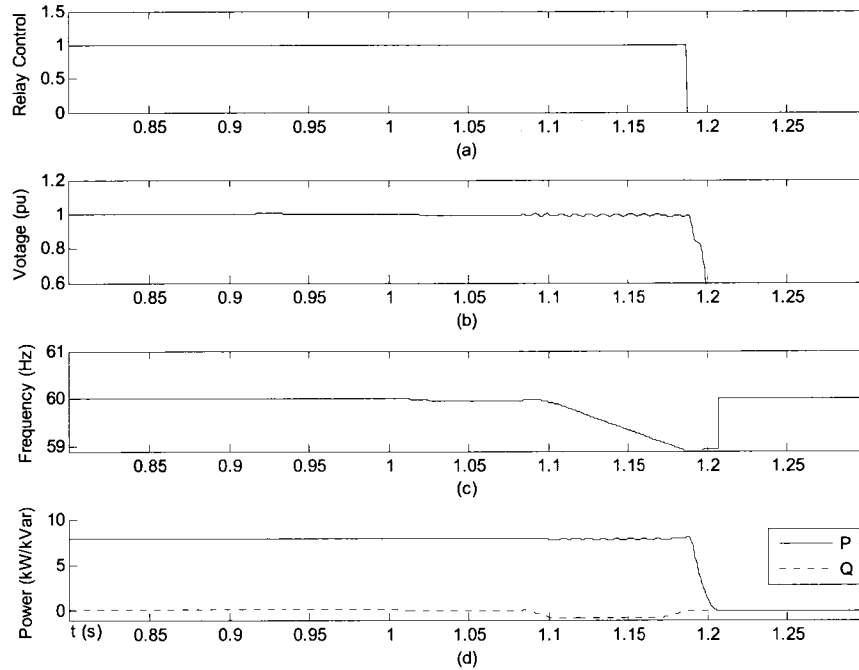


Fig. 7-7: Inverter Terminal Voltage, Frequency & Output Real and Reactive Power and Relay Control Signal (Capacitor Switching in 0.167s Period)

However, this method still has some disadvantages. The capacitor switching period must be much smaller than 2 seconds, so that the disconnecting time is within the limits of IEEE std. 1547 [32]. So if the function time of the relay is not fast enough, the switching frequency will be so high that the power losses of the capacitor and the switching impact to the feeder voltage will be noticeable. And also the size of the capacitor depends on the original NDZ of the inverter. The introduction of capacitor should not let the two temporary non detection zones overlap. Thus if the original NDZ

has a large error range in reactive power, the capacitor will also be larger which may also cause the impact to the feeder noticeable. In short, the capacitor's size and switching scheme depends highly on the inverter's size and control scheme, and it should be coordinated carefully. Otherwise, it will be unable to function or give negative impact to the power quality on the system.

## 7.2 Islanding Field Tests

This section reports the results of islanding tests that were conducted on two local grid-tied PV installations (denoted by Systems A and B). The main purpose of the experiment is to check how the inverters respond to a utility outage under the presence of a local load. PV System A is Daystar I solar facility, a fixed array type that is rated at 18 kW, and PV System B is Amonix concentrating PV system, a 2-Axis tracking concentrating array type that is rated at 25 kW. More details on these systems and the test equipments are listed Appendix III.

### 7.2.A. Test Procedure

The pieces of equipment that were used to conduct the islanding test include a load bank, a transient recorder (with voltage and current probes) that can capture voltage and current waveforms under controlled triggering, a pair of multi-meters to match the generation and load to a desired level. Due to lack of availability of an inductive load bank, only a purely resistive load (that is rated at 50 kW with a dual line voltage of 208V and 480V) was used in this test. The islanding test procedure consists of the following simple steps:

- ◆ Connect the transient recorder, load bank, and meters for reading current and power flow into the load and utility grid as shown in Fig. 7-8 below.

- ◆ Adjust the load bank to the desired load mismatch and power flow into or out of the utility grid.
- ◆ Open the utility disconnect and simultaneously record the voltage and current waveforms.
- ◆ Repeat the step above for different generation-load power mismatch levels.

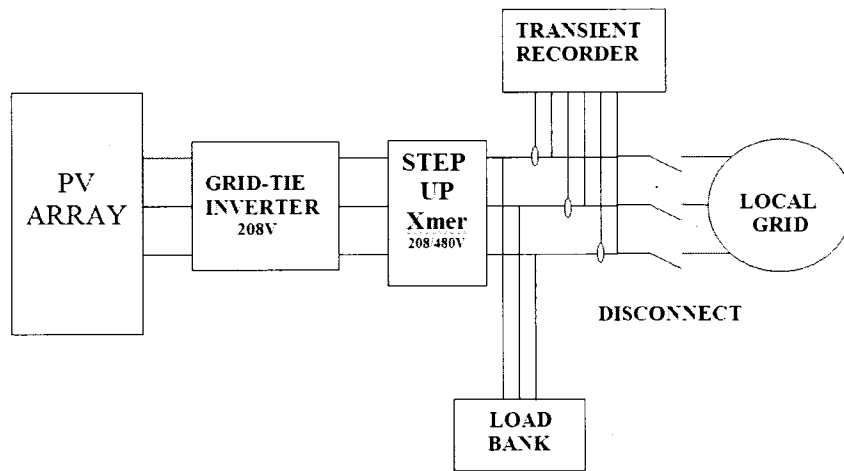


Fig. 7-8: Schematic Diagram of Test Circuit.

### 7.2.B. Test Results

It is noted that both PV systems were operating above 99% power factor (lead) during testing. More specifically, PV System A was generating nearly 15 kW and 0.9 kVAR, while PV System B was generating 20 kW and 1.2 kVAR. These reactive powers are likely generated by the shunt filter capacitors within the inverters. The utility system was disconnected numerous times under different local load conditions at each site. Some of the recorded events are presented below.

#### a) PV System A

Table 7-I below shows three utility switching events, time of event, the real power

supplied to the load bank, the real and reactive power supplied by the PV system. Event A.1 corresponds to a case where the PV system is producing nearly 3 times more power than is required by the local load. When referring to Fig. 6-1,  $P_S = -9.8$  kW (i.e.,  $\alpha = -0.66$ ) in this particular event. Fig. 7-9 shows the corresponding instantaneous phase voltages for event A.1. Note the sharp increase in peak voltages prior to inverter shutdown, an expectation that is consistent with Eqn. (6-5) that predicts a voltage a voltage rise by 70%. Eqn. (6-6) also predicts that the steady state frequency is zero since the load is purely resistive (i.e.,  $\beta = -1$ ). It appears that the over-voltage relay operated quickly before a significant decrease in frequency can be noted.

Event A.2 corresponds to a case where the PV system produces less power than local load demand ( $P_S = +4.9$  KW, and  $\alpha = +0.32$ ). In here, the voltage is expected to decrease by 13%, while the frequency is expected to again decrease to zero. The captured instantaneous voltages in Fig. 7-10 clearly show a reduction in peak value and a decrease in frequency during the last cycle prior to inverter shut-off.

Table 7-I: PV System A Switching Events.

Event No.	Switch Time (hh:mm:ss)	$P_L$ (kW)	$P_D$ (kW)	$Q_D$ (kVAR)
A.1	10:42:48	5	14.8	0.8
A.2	10:52:48	20	15.1	0.9
A.3	11:06:02	15	14.9	0.8

Finally Event A.3 corresponds to a case where the PV system real power production is nearly matched to the load ( $P_S = +0.1$  kW and  $\alpha = +0.007$ ). It should be pointed out

that perfect matching was not possible since the load can only be modified in 5 kW increments. In this event, the voltage is expected to remain constant, while the frequency drops to zero due to that small, but uncontrollable reactive power generated by the PV inverter. Fig. 7-11 shows no noticeable deviation in peak voltages or in frequency, and yet the inverter shut down within 3 and half cycles!

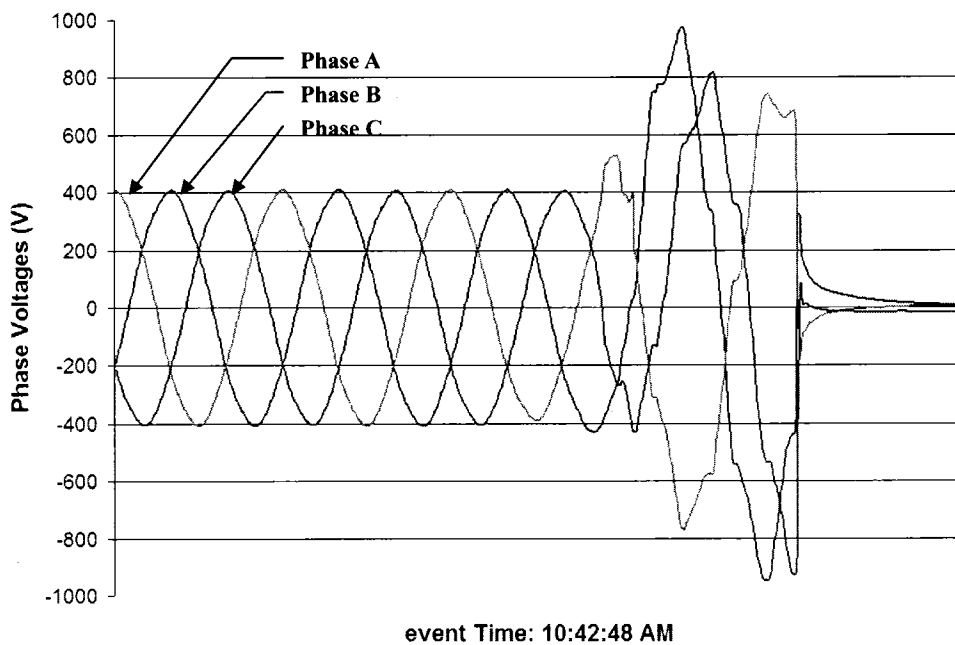
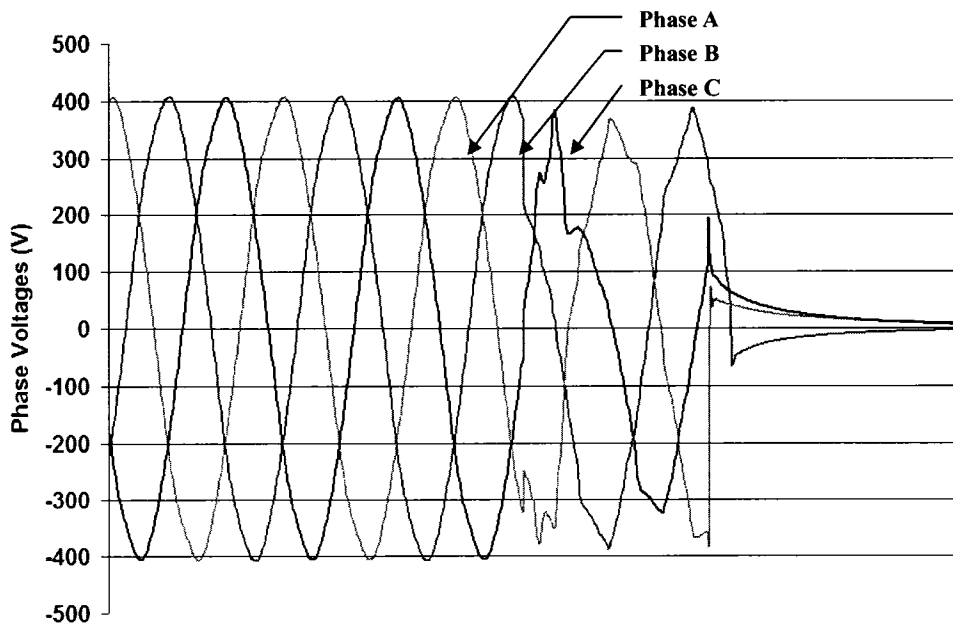
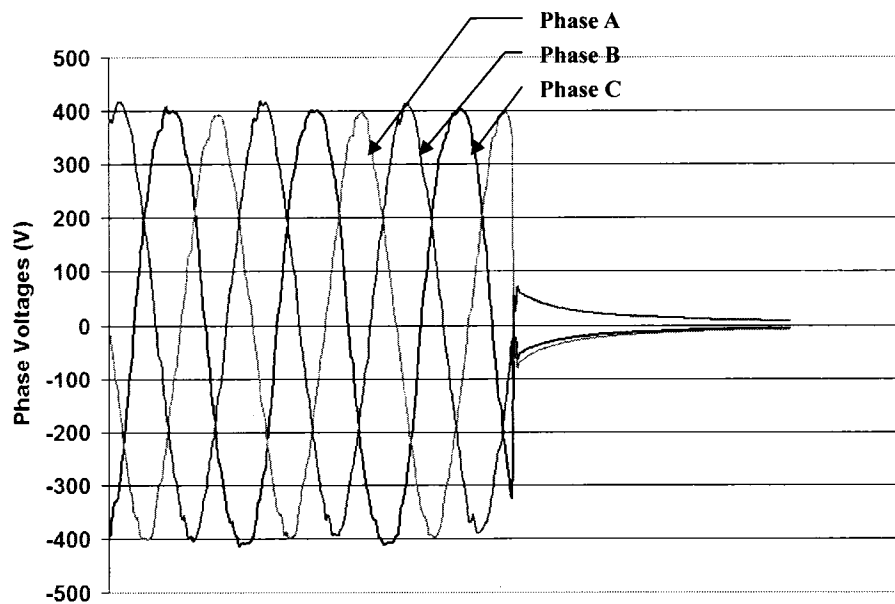


Fig. 7-9: Phase Voltage Waveforms during Event A.1.



Event Time: 10:52:48 AM

Fig. 7-10: Phase Voltage Waveforms during Event A.2.



Event Time: 11:06:02 AM

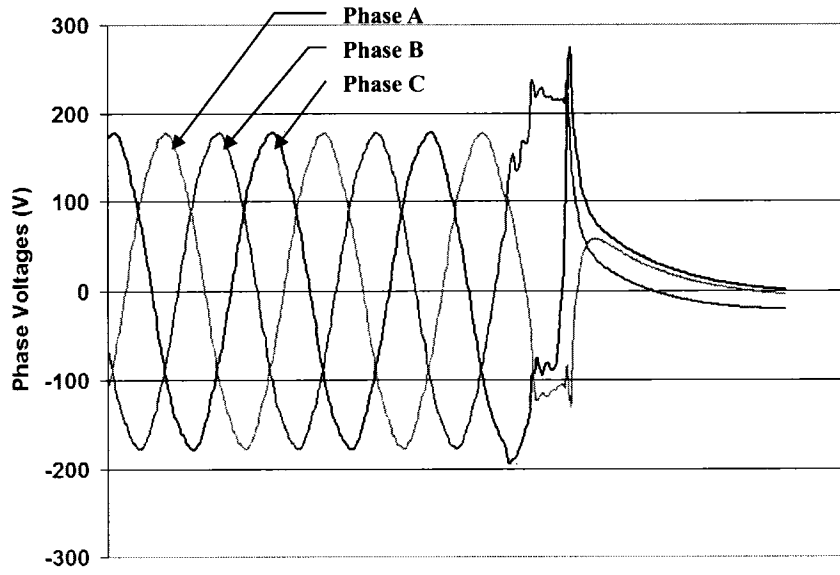
Fig. 7-11: Phase Voltage Waveforms during Event A.3.

*b) PV System B*

At the second PV plant, measurements and utility disconnect were conducted between the inverter and the 208/480 V transformer for convenience. Conducting such testing at the utility interconnection point will shut down the tracking control system, which will result in significant delays. Similar to the testing of PV System B above, Table 7-II below shows three utility switching events, and their corresponding time instants, load demand, and PV system power generation. Figs. 7-12 to 7-14 show the instantaneous phase voltages corresponding to Events B.1, B.2 and B.3, respectively.

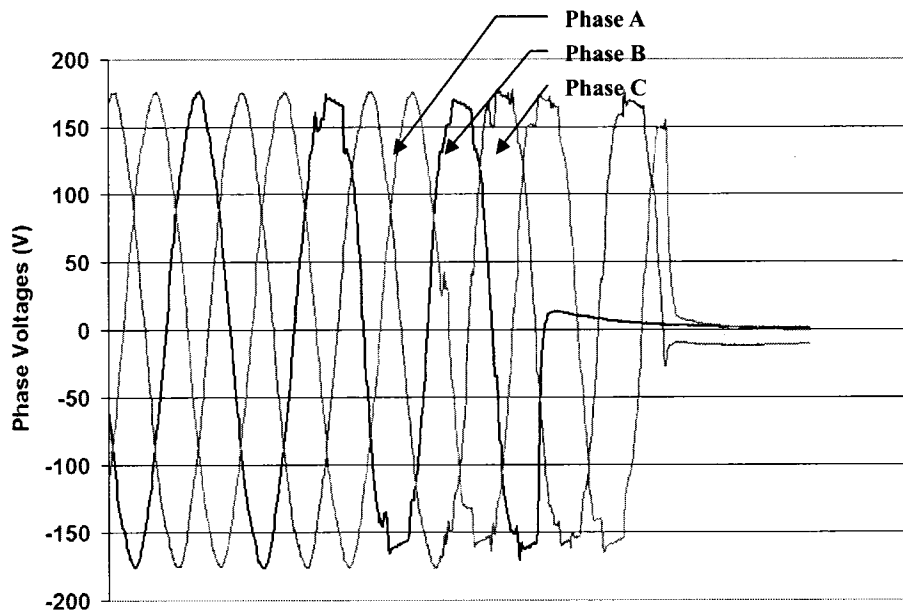
The following remarks can be made regarding the islanding test of PV System B:

- ◆ In Event B.1, the phase voltages are expected to increase by 15%. While two of the phase voltages show an increase, the third phase experienced a decrease in voltage prior to inverter shutdown.
- ◆ In Event B.2, the phase voltages are expected to decrease by 10% since the PV system is producing 81% of the local load demand. This is in agreement with the noticeable peak voltage reduction in fig. 7-13. It is also noted that one of the phases collapsed one cycle prior to the other two phases.
- ◆ In Event B.3 where the load closely matches the PV system generation, a significant drop in frequency of one of the phase voltages is noted prior to shutoff. Further, some imbalance occurred as one of the phase voltages remained active for a full cycle after the other two phases collapsed.



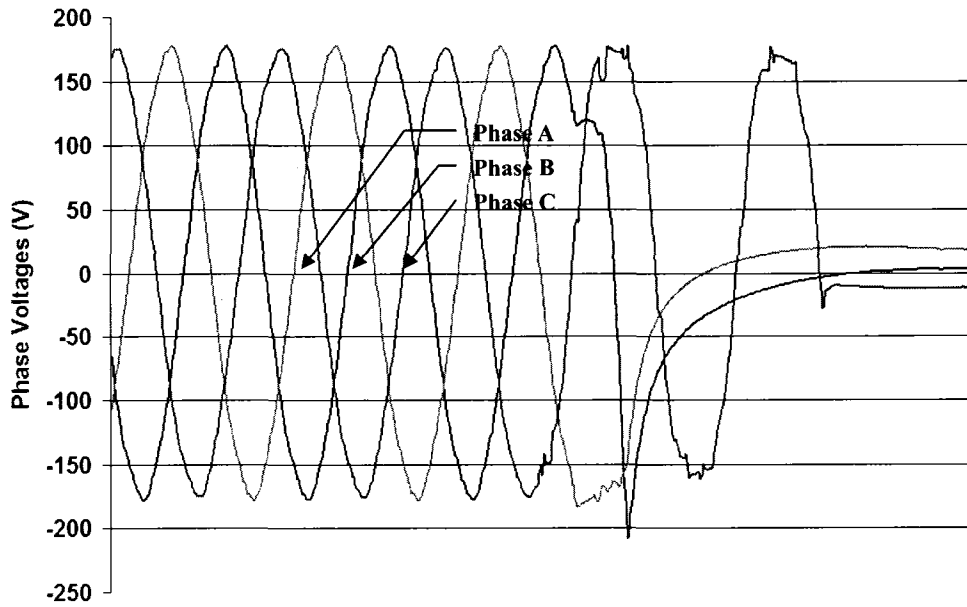
Event Time: 12:17:35 PM

Fig. 7-12: Phase Voltage Waveforms during Event B.1.



Event Time: 12:24:03 PM

Fig. 7-13: Phase Voltage Waveforms during Event B.2.



Event Time: 12:37:25 PM

Fig. 7-14: Phase Voltage Waveforms during Event B.3.

Table 7-II: PV System B Switching Events

Event No.	Switch Time (hh:mm:ss)	$P_L$ (kW)	$P_D$ (kW)	$Q_D$ (kVAR)
B.1	12:17:35	15	20.3	1.2
B.2	12:24:03	25	20.3	1.3
B.3	12:37:25	20	20.4	1.2

## CHAPTER 8

### CONCLUSION

The research work in this dissertation focused on the impact distributed generation on voltage regulation along radial feeders, and on the issue of islanding of inverter-based DG systems. The results of this research follow:

In Chapter 2, the case of installing DG unit on the radial distribution feeder is studied. It was determined that installing a DG unit leads to the possibility of experiencing over-voltages on the feeder due to excessive real and reactive power production. A simple analytical method with high accuracy is proposed to estimate the voltage profile when a DG unit is installed with specific real and reactive power output. An analytical formula was derived for the maximum DG size that can be installed at a specific location without violating voltage limits.

In Chapter 3, the case of coordinating a DG unit and the LTC transformer with LDC was analyzed. The study indicated the possibility of experiencing under-voltages towards the end of the feeder when a DG unit with significant size is installed close to the substation end. On the other hand, another regulation scheme, disabling the LDC controls and maintaining the substation voltage at the highest permissible value, may lead to over-voltages when a DG unit with significant size is installed towards the end of the feeder. As a consequence, the coordination of the installing a DG unit and the substation transformer regulation is a necessity in order to assure adequate voltage profile.

In Chapter 4, the impact of a DG unit and switched capacitors on the voltage profile was studied. The results showed that the voltage profile depends on several factors including the installed DG size and location, as well as type of capacitor controls. The study recommends revising the switched capacitor control settings to avoid voltage regulation problems.

In Chapter 5, an actual utility feeder was simulated to illustrate the voltage regulation issues in Chapters 2-4. This numerical example validated the accuracy of the analytical solutions drawn in earlier chapters, and illustrated through numerical data the cases of concern over possible under-voltages and over-voltages that might be caused by distributed generation.

In Chapter 6, a review of the conditions for possible islanding was presented, and analytical expressions of the shifts in both voltage and frequency were derived for inverter-based DGs. An elaborate MATLAB Simulink model was presented to predict the dynamic behavior of grid-tied inverter-based DG system, when a utility outage occurs.

In Chapter 7, the simulation results of the MATLAB model were presented and verified the predictions made in Chapter 6. Based on the basic model, a new simple-to-implement anti-islanding method was presented. And the simulation results show its feasibility. Field tests on two inverter-based DG systems were also conducted under various load mismatch conditions, and test results proved that the tested inverters are in compliance with current standards.

## APPENDIX I

### DEDUCTION OF EQUATION 2-2

In a circuit with only one lumped load at distance  $d$  like Fig. I-1, the relation between voltage at substation,  $V_0$ , and that at distance  $d$ ,  $V_d$ , can be illustrated as the phasor diagram like Fig.I-2.

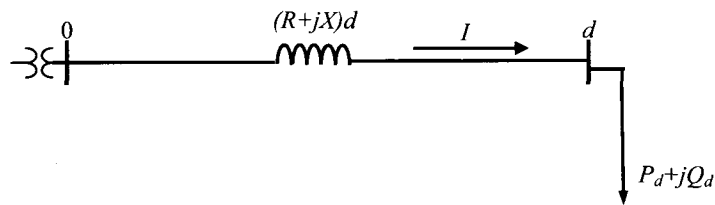


Fig. I-1: Circuit with One Lumped Load

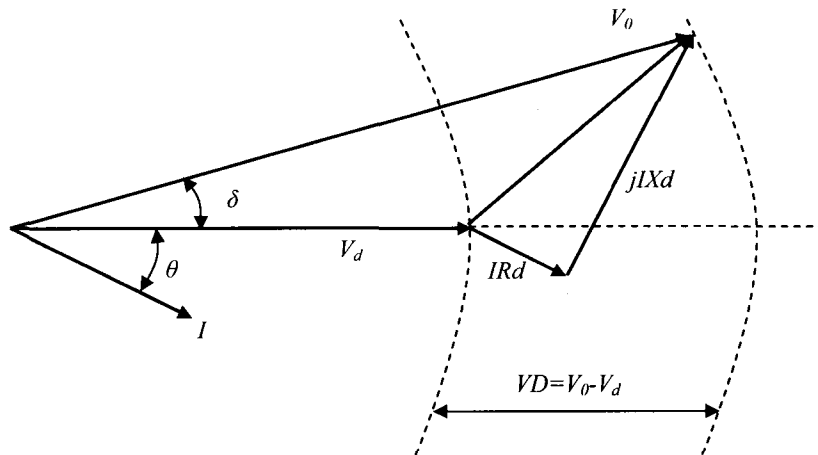


Fig. I-2: Phasor Diagram of Voltage Drop

In typical distribution system circuit, it can be found that  $R \ll X$  and  $\delta \approx 0$ . Therefore,

for a typical distribution circuit, the  $\sin \delta$  can be neglected. Hence,

$$V_0 \approx V_d \cos \delta$$

From the phasor diagram of Fig. I-2, it can be determined as

$$V_0 \approx V_d + IRd \cos \theta + IXd \sin \theta$$

Therefore the voltage drop in per unit can be represented as:

$$VD = \frac{IRd \cos \theta + IXd \sin \theta}{V_b} = d \frac{P_d R + Q_d X}{V_b^2 V_d}$$

where  $V_d$  is the per unit value and  $V_b$  is the nominal voltage of the system.

For a typical distribution system with uniformly distributed loads that looks like Fig. I-3, the voltage drop from substation to distance  $d$  can be divided into two parts: one is due to the load downstream of point  $d$ , which is  $P_d$ ; the other is due to the load upstream of point  $d$ , which is  $P_0 - P_d$ .

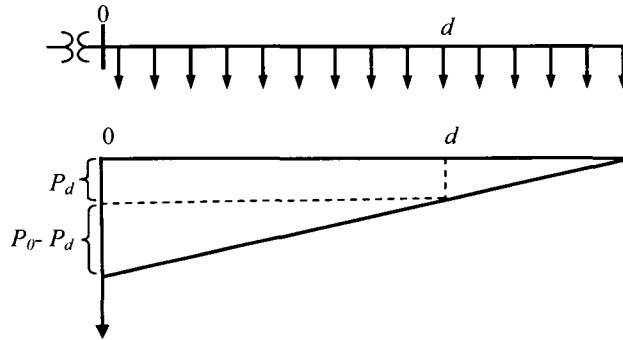


Fig. I-3: Real Power Flow Profile along the Distribution Line with Uniform Loads

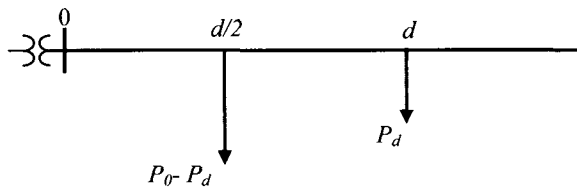


Fig. I-4: Equivalent Circuit with Two Lumped Loads

It is known these two parts of uniform loads can be equivalent to two lumped loads like Fig. I-4: one is  $P_d$  at distance  $d$  from substation; the other is  $P_0 - P_d$  at distance  $d/2$  from the substation. Getting the voltage drop due to these two lumped loads, the total voltage drop at distance  $d$  is the sum of these two parts, which is the Eqn. 2-2.

$$VD_d = d \frac{RP_d + XQ_d}{V_b^2 V_d} + \frac{d}{2} \frac{R(P_0 - P_d) + X(Q_0 - Q_d)}{V_b^2 V_d}$$

## APPENDIX II

### MATLAB SIMULINK MODEL FOR THE GRID-TIED PV SYSTEM

The grid-tied PV system is modeled as Fig. II-1. The key parts of the relay control signal generator and the PWM control signal generator are modeled as Fig. II-2 and Fig. II-3. And the model simulation monitors are modeled as Fig. II-4.

The model is working discretely at the sampling time  $T_s=5e-6$  secs. And before simulation, the model should be fed with the two input parameters:  $P_D$  and  $t_{open}$ .  $P_D$  is the nominal output real power of the PV system. And  $t_{open}$  is the time when the grid is disconnected, and it should be long enough to allow the PV system settle down to the steady state, which is set to 1 sec in this dissertation.

After the input parameters are set, the simulation can be started. Usually the simulation time can be set to 1 sec after the disconnection time of the grid,  $t_{open}$ . In this dissertation, the simulation runs 2 secs, which is long enough to show the dynamic of the circuit and the reaction of the controls and relay. And the important data, including the output real and reactive power of the PV system, the load voltage magnitude and frequency, and the control signal of the relay, are imported to the workspace after the simulation is finished. They can be used in workspace for further study.



Fig. II-2: Relay Control Signal Generator

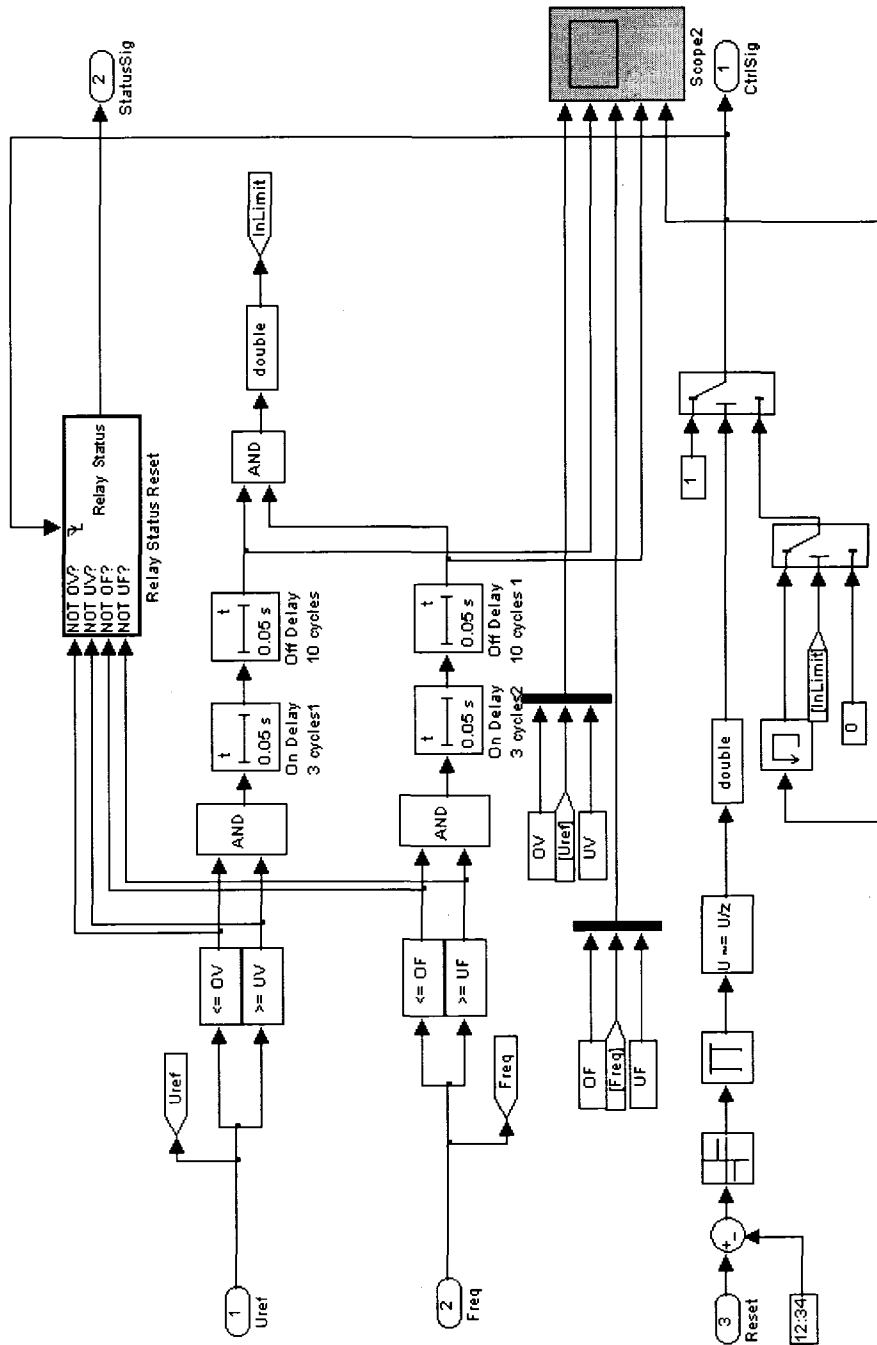


Fig. II-3: PWM Control Signal Generator

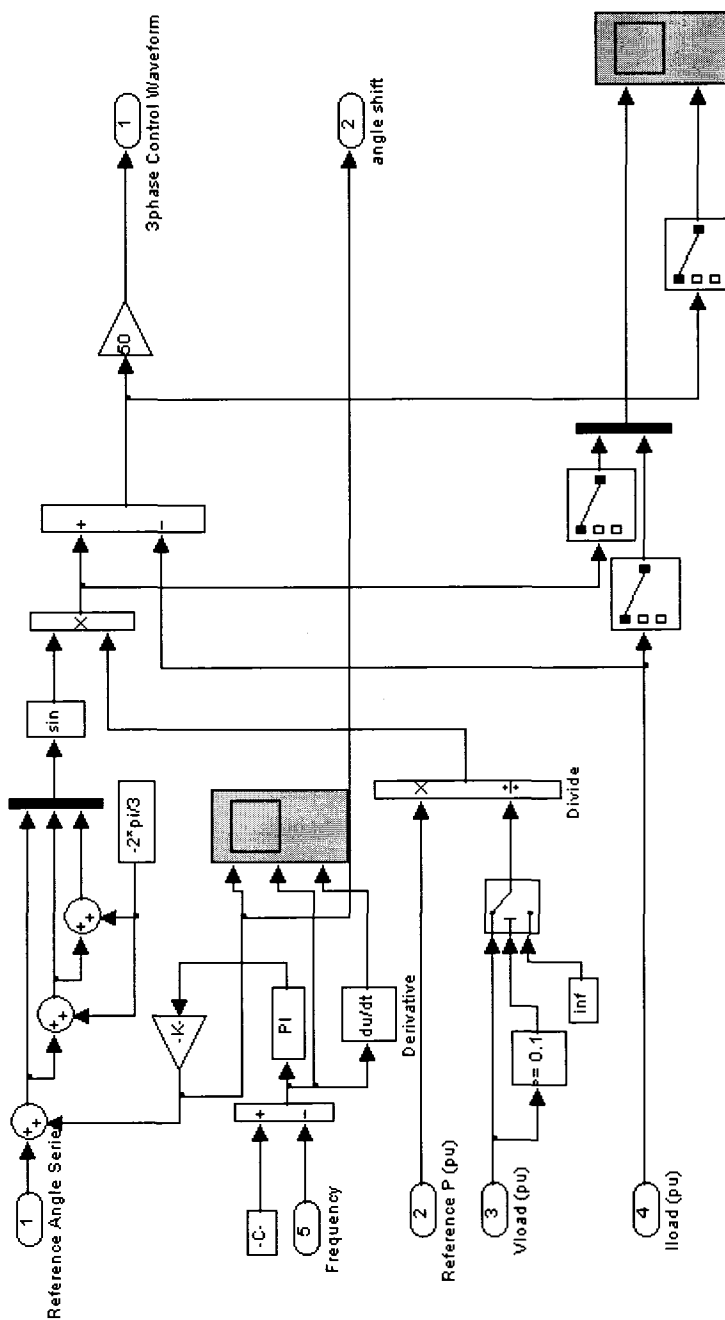
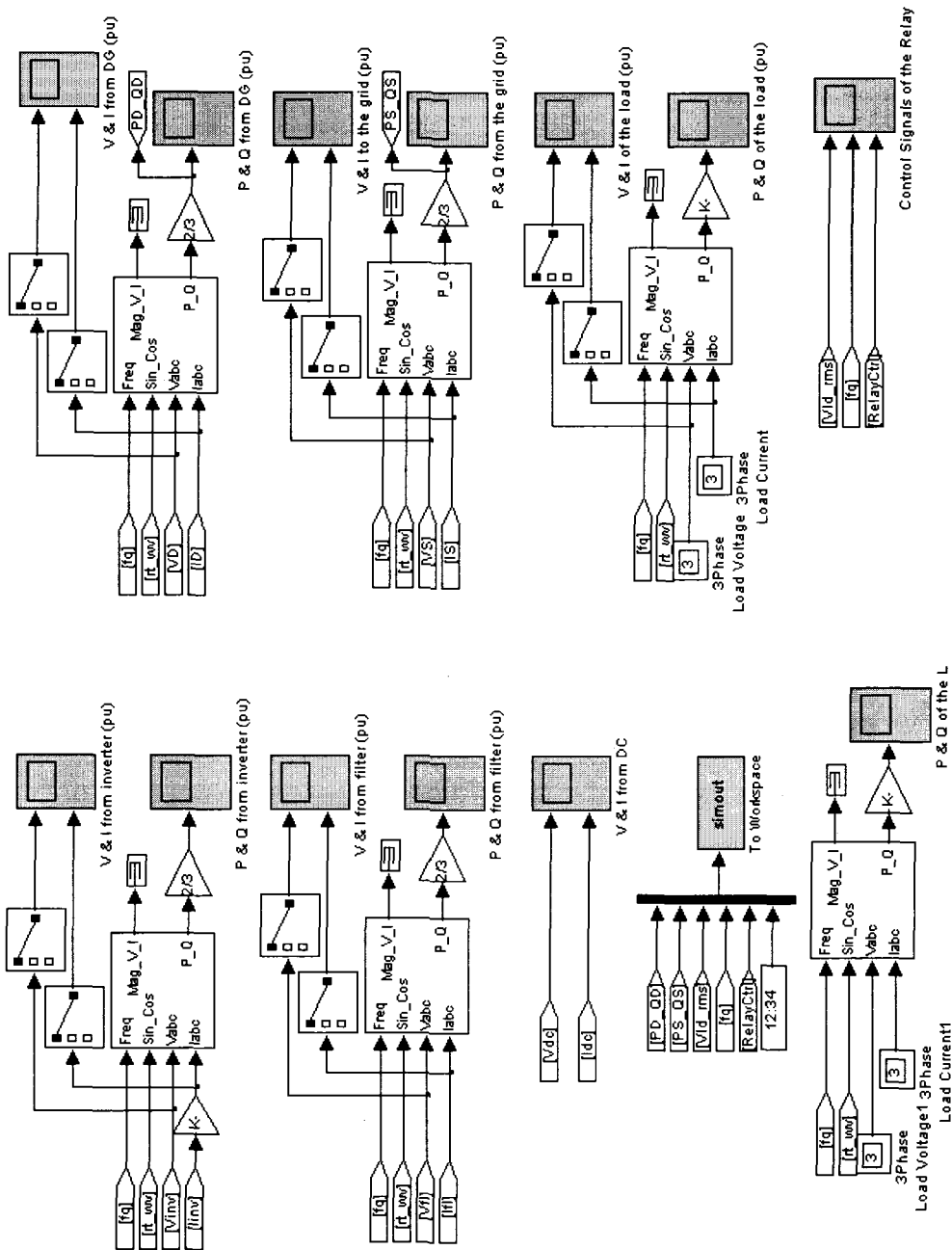


Fig. II-4 Simulation Monitor



APPENDIX III

FIELD TEST PV SYSTEMS AND EQUIPMENTS

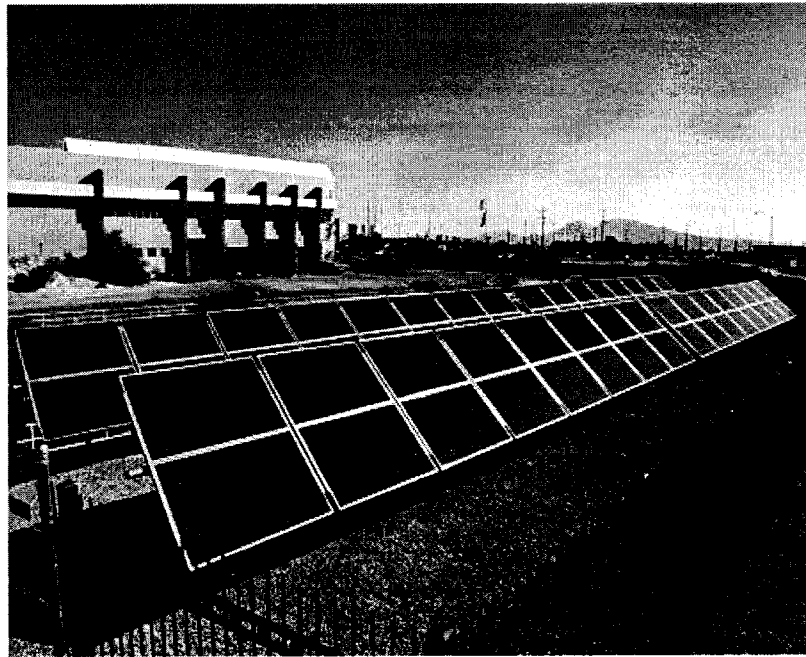


Fig. III-1: PV System A: Daystar 1 Solar Facility.

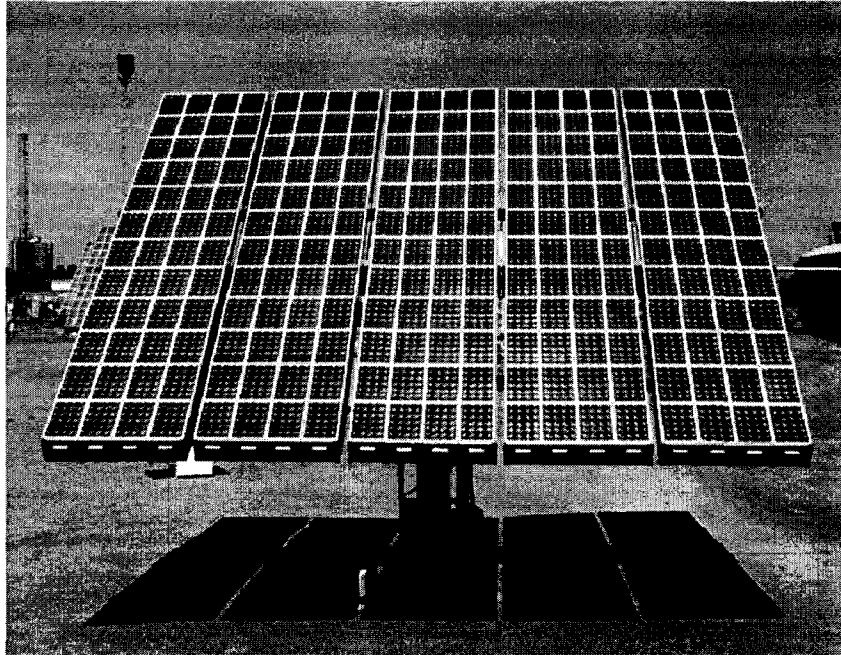


Fig. III-2: PV System B: Amonix Concentrating PV System.

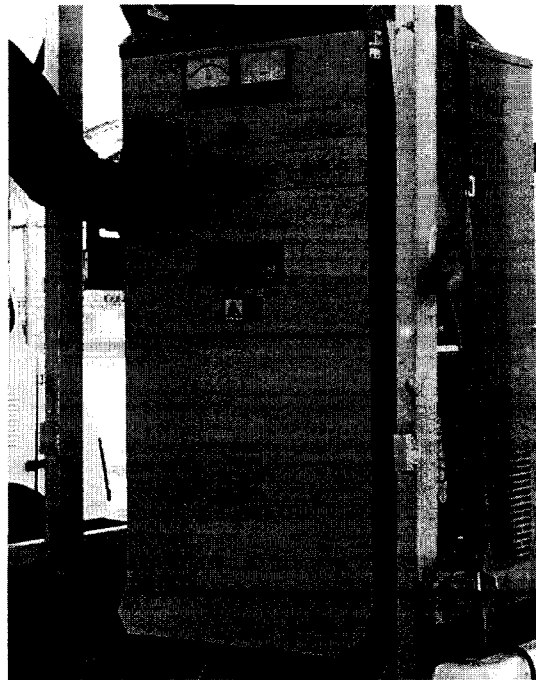


Fig. III-3: Load Bank.

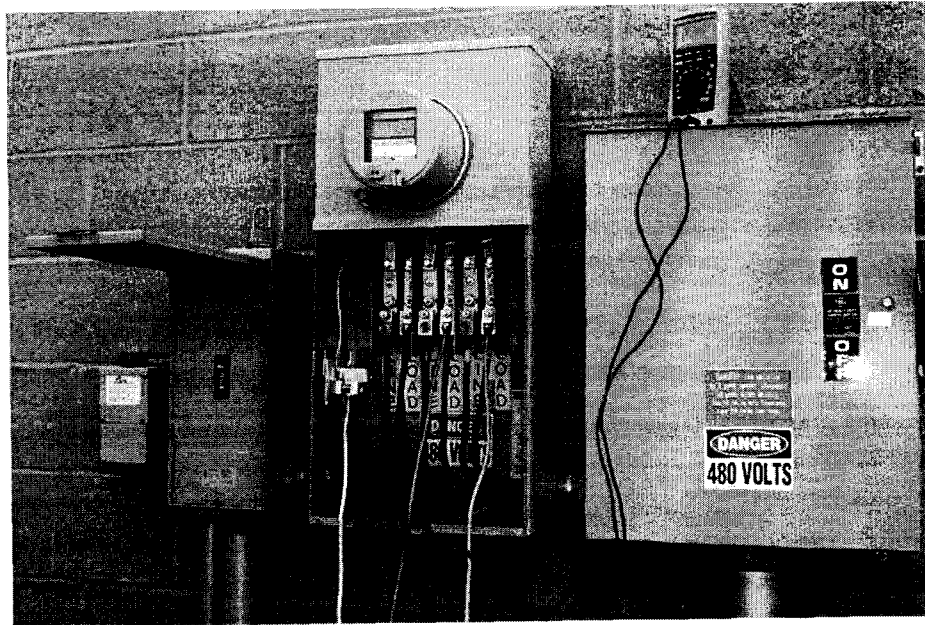


Fig. III-4: Measuring Point and Utility Disconnect Switch.

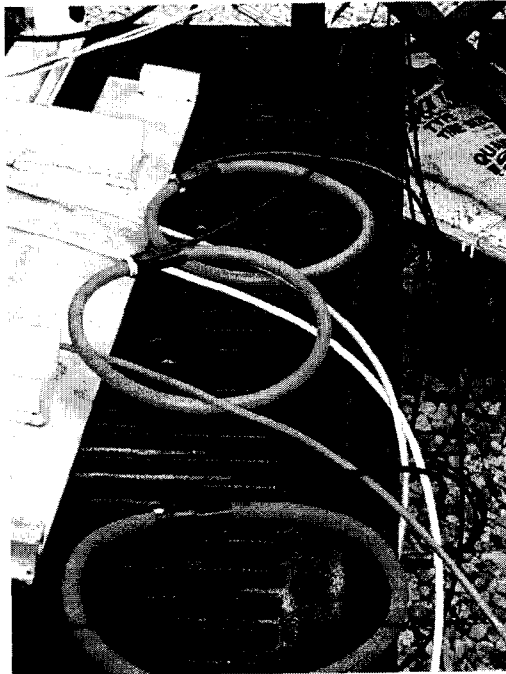


Fig. III-5: Current Probes.

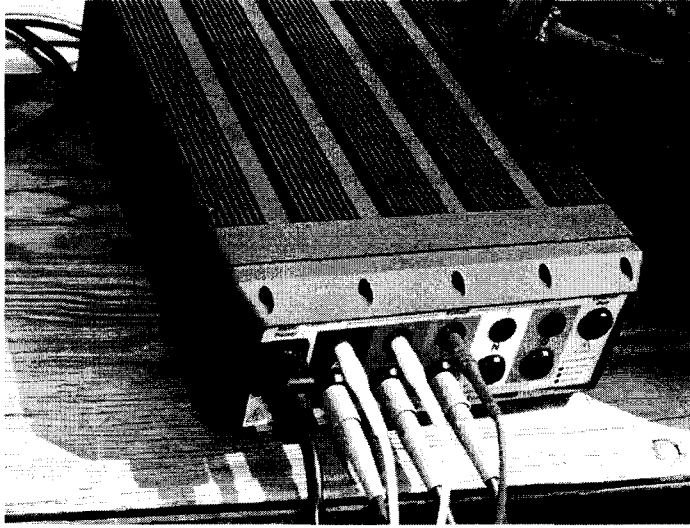


Fig. III-6: Transient Recorder.

## BIBLIOGRAPHY

- [1] U.S. Department of Energy, Office of Electric Transmission and Distribution, “‘Grid 2030’ - A National Vision for Electricity's Second 100 Year”, July 2003.
- [2] U.S. Department of Energy, “The Potential Benefits of Distributed Generation and Rate-Related Issues That May Impede Their Expansion: A Study Pursuant to Section 1817 of the Energy Policy Act of 2005”, February 2007.
- [3] EU Energy Research, Introduction to Distributed Generation, [http://ec.europa.eu/research/energy/nn/nn\\_rt/nn\\_rt\\_dg/article\\_1158\\_en.htm](http://ec.europa.eu/research/energy/nn/nn_rt/nn_rt_dg/article_1158_en.htm).
- [4] Consortium on Energy Restructuring, Virginia Tech, “Distributed Generation Education Modules”, <http://www.dg.history.vt.edu/ch1/introduction.html>.
- [5] World Alliance for Decentralized Energy (WADE), [http://www.localpower.org/ben\\_economic.html](http://www.localpower.org/ben_economic.html).
- [6] Z Ye, R. Walling, N. Miller, P. Du, K. Nelson, “Facility Microgrids”, *National Renewable Energy Laboratory*, May 2005.
- [7] G. Pepermans, J. Driesen, D. Haeseldonckx, R. Belmans, W. D'Haeseleer, “Distributed Generation: Definition, Benefits and Issues”, *Energy policy*, 2005, Vol. 33, No. 6, pp. 787-798.
- [8] California Energy Commission, “Distributed Generation and Cogeneration Policy Roadmap for California”, March 2007.
- [9] P. Dondi, D. Bayoumi, C. Haederli, D. Julian, M. Suter, “Network Integration of Distributed Power Generation”, *Journal of Power Sources*, 2002, Vol. 106, pp. 1-9.
- [10] J. Ward, et al, “Evaluation of Distributed Electric Energy Storage and Generation”, *Final Report for PSERC Project T-21, Evaluation of Distributed Electric Energy Storage and Generation*, July 2004.
- [11] U.S. Department of Energy, “Study of the Potential Benefits of Distributed Generation”, January 2006.
- [12] P.P. Barker, R. W. De Mello, “Determining the Impact of Distributed Generation on Power Systems: I. Radial Distribution Systems”, *Proc. Power Engineering Society*

*Summer Meeting*, July 2000, Vol. 3, pp.1645 - 1656.

- [13] L. Kojovic, "Impact of DG on Voltage Regulation", *Proc. IEEE/PES Summer Meeting*, July 2002, pp. 97 - 102.
- [14] R. Claire, N. Retiere, S. Martino, C. Andrieu, N. Hadjsaid, "Impact Assessment of LV Distributed Generation on MV Distribution Network", *Proc. IEEE/PES Summer Meeting*, July 2002, pp. 1423 - 1428.
- [15] P. Barker, "Over-voltage Considerations in Applying Distributed Resources on Power Systems", *Proc. IEEE/PES Summer Meeting*, July 2002, pp. 109 - 114.
- [16] T.E. Kim and J.E. Kim, "Consideration for the Feasible Operation Range of Distributed Generation Interconnected to Power Distribution system", *Proc. IEEE/PES Summer Meeting*, July 2002, pp. 42 - 48.
- [17] T.E. Kim and J.E. Kim, "A Method for Determining the Introduction Limit of Distributed Generation System in Distribution System", *Proc. IEEE/PES Summer Meeting*, July 2001, pp. 456 - 461.
- [18] T.E. Kim and J.E. Kim, "Voltage Regulation Coordination of Distributed Generation System in Distribution System", *Proc. IEEE/PES Summer Meeting*, July 2001, pp. 480 - 484.
- [19] J.H. Choi, J.C. Kim, "Advanced Voltage Regulation Method at the Power Distribution Systems Interconnected with Dispersed Storage and Generation Systems", *IEEE Trans. Power Delivery*, Vol. 15, No. 2, April 2000, pp. 691-696.
- [20] H.L. Willis, "Analytical Methods and Rules of Thumb for Modeling DG – Distribution Interaction", *Proc. IEEE/PES Summer Meeting*, July 2000, pp. 1643 - 1644.
- [21] S. Conti, S. Raiti, G. Tina, U. Vagliasindi, "Study of the Impact of PV Generation on Voltage Profile in LV Distribution Networks", *Proc. IEEE Porto Power Tech Conference*, September 2001, Vol. 4, pp. 1-6.
- [22] IEEE Std. 929-2000, "Recommended Practice for Utility Interface of Photovoltaic (PV) Systems", *IEEE Press*, 2000.
- [23] J. Stevens, R. Bonn, J. Ginn, S. Gonzalez, "Development and Testing of an Approach to Anti-Islanding in Utility-Interconnected Photovoltaic Systems", *Sandia National Laboratories*, Report No. SAND 2000-1939, August 2000.
- [24] S. Gonzalez, R. Bonn, J. Ginn, "Removing Barriers to Utility Interconnected Photovoltaic Inverters", *Proc. 28<sup>th</sup> IEEE Photovoltaic Specialist Conference*,

September 2000, pp. 1691 -1694.

- [25] L.K. Kumpulainen, K.T. Kauhaniemi, "Analysis of the Impact of Distributed Generation on Automatic Reclosing", *Proc. IEEE PES Power Systems Conference and Exposition*, October 2004, Vol.1, pp. 603 - 608.
- [26] H.L. Willis, "Power Distribution Planning Reference Book", *Marcel Dekker Inc.*, 1997.
- [27] T. Gonen, "Electric Power Distribution System Engineering", *McGraw-Hill Book Company*, 1986.
- [28] J.J. Grainger, S.H. Lee, "Optimum Size and Location of Shunt Capacitors for Reduction of Losses on Distribution Feeders", *IEEE Trans. Power Apparatus and Systems*, Vol. PAS-100, No. 3, 1981, pp. 1105-1112
- [29] D. Jiang, R. Baldik, "Optimal Electric Distribution System Switch Reconfiguration and Capacitor Control", *IEEE Trans. Power Delivery*, Vol. 11, No. 2, 1996, pp. 890 - 897.
- [30] E. Lakervi, E.J. Holmes, "Electricity Distribution Network Design," *IEE Power Engineering Series*, 2003.
- [31] IEEE Std. 519-1992, "IEEE Recommended Practices and Requirements for Harmonic Control in Electrical Power Systems –Description", *IEEE Press*, June 2004.
- [32] IEEE P1547, "Standard for Distributed Resources Interconnected with Electric Power Systems, Draft 10", *IEEE Press*, January 2003.
- [33] M.E. Ropp, K. Aaker, J. Haigh, N. Sabbah, "Using Power Line Carrier Communications To Prevent Islanding", *Proc. 28<sup>th</sup> IEEE Photovoltaics Specialists Conference*, September 2000, pp. 1675-1678.
- [34] T. Ishida, R. Hagihara, M. Yugo, Y. Makino, M. Maekawa, A. Takeoka, R. Susuzi, S. Nakano, "Anti-Islanding Protection Using a Twin-Peak Band-Pass Filter in Interconnected PV Systems, and Substantiating Evaluations", *Proc. 24<sup>th</sup> IEEE Photovoltaics Specialists Conference*, December 1994, pp. 1077 –1080.
- [35] M.E. Ropp, M. Begovic, A. Rohatgi, "Prevention of Islanding in Grid-tied Photovoltaic Systems", *Progress in Photovoltaics Research and Applications*, 1999, Vol. 7, pp. 39-59.
- [36] M. Begovic, M. E. Ropp, A. Rohatgi, "Determining the Sufficiency of Standard

Protective Relaying for Islanding Prevention in Grid-connected PV Systems”, *Proc. 2<sup>nd</sup> World Conference on Photovoltaic Energy Conversion*, May 1998, pp. 2519 - 2522.

- [37] A. Ye, A. Kolwalkar, Y. Zhang, P. Du, R. Walling, “Evaluation of Anti-Islanding Schemes Based on Non-detection Zone Concept”, *IEEE Trans. Power Electronics*, Vol. 19, No. 5, September 2004, pp. 1171-1176.
- [38] W. Xu, K. Mauch, S. Martel, "An Assessment of Distributed Generation Islanding Detection Methods and Issues for Canada", *Report No. CETC – Varennes 2004-074*, CANMET Energy Technology Centre – Varennes, August 2004.
- [39] H.H. Zeineldin, E.F. El-Saadany, M.M.A. Salama, “Impact of DG Interface Control on Islanding Detection and Nondetection Zones”, *IEEE Tran. Power Delivery*, Vol. 21, July 2006, pp.1515 – 1523.
- [40] S.I. Jang, K.H. Kim, “An Islanding Detection Method for Distributed Generations Using Voltage Unbalance and Total Harmonic Distortion of Current”, *IEEE Trans. Power Delivery*, Vol. 19, April 2004, pp.745 – 752.
- [41] H. Zeineldin, E.F. El-Saadany, M.M.A. Salama, “Impact of DG Interface Control on Islanding Detection”, *Proc. IEEE Power Engineering Society General Meeting*, June 2005, Vol. 2, pp.1489 - 1495.
- [42] L. Asiminoaei, R. Teodorescu, F. Blaaberg, U. Borup, “A New Method of On-line Grid Impedance Estimation for PV Inverter”, *Proc. 19<sup>th</sup> Annual IEEE Applied Power Electronics Conference*, 2004, pp. 1527 – 1533.
- [43] K.W. Koeln, “Method and Device for Measuring Impedance in Alternating Current Networks and Method and Device for Preventing the Formation of Separate Networks”, *European Patent EP0783702-B*, 1999.
- [44] Y. Baghzouz, “Effect of Grid-Tied Photovoltaic Systems of System Reliability and Peak Demand”, *Proc. International Conference on Energy for Sustainable Development*, March 2006, WIII-19, p. 4.
- [45] E.J. Coster, A. Ishchenko, J.M.A. Myrzik, W.L. Kling, “Modeling, Simulating and Validating Wind Turbine Behavior During Grid Disturbances”, *Proc. IEEE Power Engineering Society General Meeting*, June 2007, pp. 1-6.
- [46] G. Venkataramanan, B. Wang, “Dynamic modeling and control of three phase pulse width modulated power converters using phasors”, *Proc. IEEE 35<sup>th</sup> Annual Power Electronics Specialists Conference*, 2004, Vol. 4, pp. 2822 – 2828.

- [47] E.F.M. Kheswa, I.E. Davidson, "Model of a photovoltaic fuel-cell generator", *Proc. 7<sup>th</sup> AFRICON Conference in Africa*, 2004, Vol. 2, pp. 735 – 739.
- [48] W. El-Khattam, Y. Hegazy, M. Salama, "An integrated distributed generation optimization model for distribution system planning", *Proc. IEEE Power Engineering Society General Meeting*, June 2005, Vol.3, pp. 2392.
- [49] H. Li; Y. Li; Z. Li, "A Multiperiod Energy Acquisition Model for a Distribution Company With Distributed Generation and Interruptible Load", *IEEE Transactions on Power Systems*, Vol. 22, Issue 2, May 2007, pp. 588 – 596.
- [50] R. Palma-Behnke, L.S. Vargas, A. Jofre, "A distribution company energy acquisition market model with integration of distributed generation and load curtailment options", *IEEE Transactions on Power Systems*, Vol. 20, Issue 4, November 2005, pp. 1718 – 1727.
- [51] M.T. Doyle, "Reviewing the impacts of distributed generation on distribution system protection", *Proc. IEEE Power Engineering Society Summer Meeting*, July 2002, Vol. 1, pp. 103 – 105.
- [52] W. El-Khattam, M. Elnady, M.M.A. Salama, "Distributed generation impact on the dynamic voltage restorer rating", *Proc. IEEE PES Transmission and Distribution Conference and Exposition*, September 2003, Vol. 2, pp. 595 – 599.
- [53] K. Kauhaniemi, L. Kumpulainen, "Impact of distributed generation on the protection of distribution networks", *Proc. 8<sup>th</sup> IEE International Conference on Developments in Power System Protection*, April 2004, Vol. 1, pp. 315 – 318.
- [54] C. Dai, Y. Baghzouz, "Impact of Distributed Generation on Voltage Regulation by LTC Transformer", *Proc. IEEE ICHQP XI*, Lake Placid, NY, October 2004, pp. 1136 - 1140.
- [55] P. Brady, C. Dai, Y. Baghzouz, "Need to Modify Switched Capacitor Controls on Feeders with Distributed Generation", *Proc. IEEE/PES T&D Conference*, Dallas, TX, September 2003, pp. 590 - 594.
- [56] C. Dai, Y. Baghzouz, "On the Voltage Profile of Distribution Feeders with Distributed Generation", *Proc. 2003 IEEE/PES General Meeting*, July 2003, pp. 770 – 773.

- [57] Y. Baghzouz, "Islanding Test Results of Some Local Grid-Tied Photovoltaic Systems", *Proc. International Conference on Energy for Sustainable Development*, March 2006, WIII-15, p. 4.

VITA

Graduate College  
University of Nevada, Las Vegas

Chensong Dai

Local Address:

1600 E. University Ave. #130,  
Las Vegas, Nevada 89119

Home Address:

AnDunXinYu Bldg. 8, Rm. 502, HeHuaChi Rd.,  
Yangzhou, Jiangsu, 225009, China PR.

Degree:

Bachelor of Electrical Engineering, 1997  
Tsinghua University, China

Master of Electrical Engineering, 2000  
Nanjing Automation Research Institute, China

Publications:

"Impact of Distributed Generation on Voltage Regulation by LTC Transformer", *Proc. IEEE ICHQP XI*, October 2004.

"Need to Modify Switched Capacitor Controls on Feeders with Distributed Generation", *Proc. IEEE/PES T&D Conference*, September 2003.

"On the Voltage Profile of Distribution Feeders with Distributed Generation", *Proc. 2003 IEEE/PES General Meeting*, July 2003.

Dissertation Title: A Study of Voltage Regulation and Islanding Associated with Distributed Generation

Dissertation Examination Committee:

Chairperson, Dr. Yahia Baghzouz, Ph. D.

Committee member, Dr. Robert A. Schill, Ph. D.

Committee member, Dr. Yingtao Jiang, Ph.D.

Graduate Faculty Representative, Dr. Laxmi P. Gewali, Ph.D.